Madsen, O.D. (2000b) Control of endodermal endocrine development by Hes-1. Nat Genet 24:36–44.

Juven-Gershon, T., Shifman, O., Unger, T., Elkeles, A., Haupt, Y. and Oren, M. (1998) The Mdm2 oncoprotein interacts with the cell fate regulator Numb. Mol Cell Biol 18:3974–3982.

Krebs, L.T., Xue, Y., Norton, C.R., Shutter, J.R., Maguire, M., Sundberg, J.P., Gallahan, D., Closson, V., Kitajewski, J., Callahan, R., Smith, G.H., Stark, K.L. and Gridley, T. (2000) Notch signaling is essential for vascular morphogenesis in mice. Genes Dev 14:1343–1352.

Lammert, E., Brown, J. and Melton, D.A. (2000) Notch gene expression during pancreatic organogenesis. Mech Dev 94:199–203.

Lu, B., Jan, L. and Jan, Y.N. (2000) Control of cell divisions in the nervous system: symmetry and asymmetry. Annu Rev Neurosci 23:531–556.

Nie, J., McGill, M.A., Dermer, M., Dho, S.E., Wolting, C.D. and McGlade, C.J. (2002) LNX functions as a RING type E3 ubiquitin ligase that targets the cell fate determinant Numb for ubiquitin-dependent degradation. EMBO J 21:93–102.

Pang, K., Mukonoweshuro, C. and Wong, G.G. (1994) β cells arise from glucose transporter type 2 (Glut2)-expressing epithelial cells of the developing rat pancreas. Proc Natl Acad Sci USA 91:9559–9563.

Petersen, P.H., Zou, K., Hwang, J.K., Jan, Y.N. and Zhong, W. (2002) Progenitor cell maintenance requires numb and numblike during mouse neurogenesis. Nature 419:929–934.

Schwitzgebel, V.M., Scheel, D.W., Conners, J.R., Kalamaras, J., Lee, J.E., Anderson, D.J., Sussel, L., Johnson, J.D. and German, M.S. (2000) Expression of neurogenin3 reveals an islet cell precursor population in the pancreas. Development 127:3533–3542.

Sestan, N., Artavanis-Tsakonas, S. and Rakic, P. (1999) Contact-dependent inhibition of cortical neurite growth mediated by notch signaling. Science 286:741–746.

Slack, J.M. (1995) Developmental biology of the pancreas. Development 121:1569–1580.

Susini, L., Passer, B.J., Amzallag-Elbaz, N., Juven-Gershon, T., Prieur, S., Privat, N., Tuynder, M., Gendron, M.C., Israel, A., Amson, R., Oren, M. and Telerman, A. (2001) Siah-1 binds and regulates the function of Numb. Proc Natl Acad Sci USA 98:15067–15072.

Swenne, I. (1992) Pancreatic β-cell growth and diabetes mellitus. Diabetologia 35:193–201.

Uemura, T., Shepherd, S., Ackerman, L., Jan, L.Y. and Jan, Y.N. (1989) numb, a gene required in determination of cell fate during sensory organ formation in *Drosophila* embryos. Cell 58:349–360.

Verdi, J.M., Bashirullah, A., Goldhawk, D.E., Kubu, C.J., Jamali, M., Meakin, S.O. and Lipshitz, H.D. (1999) Distinct human NUMB isoforms regulate differentiation vs. proliferation in the neuronal lineage. Proc Natl Acad Sci USA 96: 10472–10476.

Wakamatsu, Y., Maynard, T.M., Jones, S.U. and Weston, J.A. (1999) NUMB localizes in the basal cortex of mitotic avian neuroepithelial cells and modulates neuronal differentiation by binding to NOTCH-1. Neuron 23:71–81.

Zhong, W., Feder, J.N., Jiang, M.M., Jan, L.Y. and Jan, Y.N. (1996) Asymmetric localization of a mammalian numb homolog during mouse cortical neurogenesis. Neuron 17:43–53.

Zhong, W., Jiang, M.M., Weinmaster, G., Jan, L.Y. and Jan, Y.N. (1997) Differential expression of mammalian Numb, Numblike and Notch1 suggests distinct roles during mouse cortical neurogenesis. Development 124:1887–1897.

Zilian, O., Saner, C., Hagedorn, L., Lee, H.Y., Sauberli, E., Suter, U., Sommer, L. and Aguet, M. (2001) Multiple roles of mouse Numb in tuning developmental cell fates. Curr Biol 11:494–501.

Cell, Vol. 115, 163–175, October 17, 2003, Copyright ©2003 by Cell Press

F3/Contactin Acts as a Functional Ligand for Notch during Oligodendrocyte Maturation

Qi-Dong Hu,[1,2] Beng-Ti Ang,[1,2,3,16] Meliha Karsak,[4,16] Wei-Ping Hu,[5,16] Xiao-Ying Cui,[1,16] Tanya Duka,[1] Yasuo Takeda,[6] Wendy Chia,[1] Natesan Sankar,[7] Yee-Kong Ng,[2] Eng-Ang Ling,[2] Thomas Maciag,[8] Deena Small,[8] Radianna Trifonova,[8] Raphael Kopan,[9] Hideyuki Okano,[10] Masato Nakafuku,[11] Shigeru Chiba,[12] Hisamaru Hirai,[12] Jon C. Aster,[13] Melitta Schachner,[4] Catherine J. Pallen,[14] Kazutada Watanabe,[6,15,*] and Zhi-Cheng Xiao[1,2,*]

[1]Department of Clinical Research
Singapore General Hospital
169608 Singapore
[2]Department of Anatomy
National University of Singapore
117597 Singapore
[3]Department of Neurosurgery
National Neuroscience Institute
306433 Singapore
[4]Zentrum fur Molekulare Neurobiologie
University of Hamburg
Hamburg 20251, Germany
[5]Department of Obstetrics and Gynecology
Singapore General Hospital
169608 Singapore
[6]Department of Cell Recognition
Tokyo Metropolitan Institute of Gerontology
Tokyo 173-0015, Japan
[7]National Cancer Center
169610 Singapore
[8]Center for Molecular Medicine
Maine Medical Center Research Institute
Scarborough, Maine 04469
[9]Department of Molecular Biology and Pharmacology and the Department of Medicine
Division of Dermatology
Washington University School of Medicine
St. Louis, Missouri 63110
[10]Department of Physiology
Keio University School of Medicine
Tokyo 160-8582, Japan
[11]Department of Neurobiology
The University of Tokyo Graduate School of Medicine
Tokyo 113-0033, Japan
[12]Departments of Cell Therapy, Transplantation Medicine and Hematology, and Oncology
University of Tokyo
Tokyo 113-8655 Japan
[13]Department of Pathology
Brigham and Women's Hospital
Harvard Medical School
Boston, Massachusetts 02115
[14]Department of Pediatrics
University of British Columbia
BC Research Institute for Children's and Women's Health
Vancouver, British Columbia V5Z 4H4, Canada
[15]Department of Bioengineering
Nagaoka University of Technology
Nagaoka 9402188, Japan

*Correspondence: gcrxzc@sgh.com.sg (Z.C.X.), kazutada@vos.nagaokaut.ac.jp (K.W.)
[16]These authors contributed equally to this work.

Summary

Axon-derived molecules are temporally and spatially required as positive or negative signals to coordinate oligodendrocyte differentiation. Increasing evidence suggests that, in addition to the inhibitory Jagged1/Notch1 signaling cascade, other pathways act via Notch to mediate oligodendrocyte differentiation. The GPI-linked neural cell recognition molecule F3/contactin is clustered during development at the paranodal region, a vital site for axoglial interaction. Here, we show that F3/contactin acts as a functional ligand of Notch. This *trans*-extracellular interaction triggers γ-secretase-dependent nuclear translocation of the Notch intracellular domain. F3/Notch signaling promotes oligodendrocyte precursor cell differentiation and upregulates the myelin-related protein MAG in OLN-93 cells. This can be blocked by dominant negative Notch1, Notch2, and two Deltex1 mutants lacking the RING-H2 finger motif, but not by dominant-negative RBP-J or Hes1 antisense oligonucleotides. Expression of constitutively active Notch1 or Notch2 does not upregulate MAG. Thus, F3/contactin specifically initiates a Notch/Deltex1 signaling pathway that promotes oligodendrocyte maturation and myelination.

Introduction

Myelination in the vertebrate central nervous system (CNS) is essential for rapid impulse conduction. Studies of oligodendrocyte precursors (OPCs) in conditional Notch1 null mice reveal ectopic immature oligodendrocytes (OLs) in the CNS (Genoud et al., 2002). Rapid generation of OLs and concomitant myelination of rat retinal ganglion cell axons parallels the sharp decrease of the axonal ligand of Notch, Jagged1, which commences around postnatal day 6 (P6) (Wang et al., 1998), suggesting that Jagged1/Notch interaction inhibits OPC differentiation. However, the molecular mechanisms timing OPC differentiation to OLs and subsequent OL maturation remain poorly defined.

Notch is a type I transmembrane protein mediating cell fate selection via lateral inhibition. Its core signaling mechanism involves *R*egulated *I*ntramembrane *P*roteolysis (RIP) (Ebinu and Yankner, 2002). Upon binding the classic ligands, *D*elta, *S*errate/Jagged and *L*ag-2 (collectively called DSL), Notch undergoes two proteolytic cleavages that release its intracellular domain (NICD). NICD translocates to the nucleus and interacts with RBP-J transcription factor to activate, for instance, *Hes* genes (Martinez Arias et al., 2002). In addition, Deltex1

(DTX1) has been identified as a cytoplasmic downstream element of the Notch signaling pathway. DTX homologs share three common domains, namely, the N-terminal region and the proline-rich and RING-H2 finger motifs (Kishi et al., 2001). Particularly, the N-terminal region interacts with NICD. Notch signaling via DTX1 represses JNK signaling, a pathway regulating OL differentiation, and cooperates with Wingless signaling (Martinez Arias et al., 2002). Although several studies imply the existence of an extracellular ligand that activates Notch/DTX1 signaling, the putative ligand has not yet been identified.

F3/contactin is a glycosyl phosphatidylinositol (GPI)-anchored neural cell adhesion molecule of the immunoglobulin superfamily (Revest et al., 1999). It is a neuronal receptor for the oligodendrocyte-related extracellular matrix glycoprotein tenascin-R via epidermal growth factor (EGF)-like repeats (Xiao et al., 1996). F3 interacts in *trans* with RPTPζ/β (receptor protein tyrosine phosphatase) to promote neurite outgrowth (Sakurai et al., 1997) and in *cis* with RPTPα (Zeng et al., 1999) to transduce extracellular signals to myelination-related Fyn kinase (Umemori et al., 1994). Additionally, F3 colocalizes and interacts in *cis* with Caspr/Paranodin and in *trans* with glial neurofascin 155 at the paranode (Girault and Peles, 2002), a key site of axoglial contact for myelination. F3 null mice exhibit partially disrupted paranodal structure and die by P18 (Berglund et al., 1999), suggesting that F3 may be critical for development. In the present study, we demonstrate that F3 is a physiological ligand of Notch and that the signaling via DTX1 promotes OL development.

Results

Notch Is the Oligodendroglial Surface Binding Partner of F3

Axonal F3 congregates at the paranode, a potential site for F3 to interact with myelinating glia (Girault and Peles, 2002). Notch is a plausible binding partner since its extracellular portion possesses many EGF-like repeats (Martinez Arias et al., 2002) and is abundantly expressed on maturing OLs (Lardelli et al., 1994; Wang et al., 1998). To investigate this potential interaction, we utilized an OL cell line OLN-93 (OLN) that was derived from spontaneously transformed cells in rat brain glial cultures and resembles maturing OLs (Richter-Landsberg and Heinrich, 1996). OLN cells no longer express the progenitor cell surface marker A2B5, and are positive for only one isoform of myelin basic protein (MBP) (~14 kDa), characteristic of immature OLs. Immunocytochemistry confirmed that OLN cells express Notch1 and Notch2 on their surface (Figures 1Aa and 1Ab).

To investigate if F3 could bind to Notch, we first performed cell adhesion assays (Xiao et al., 1996). After plating, OLN cells adhered readily to F3 substrate (Figure 1Ac), but not to CHL1-Fc (CHL1), another neural cell adhesion molecule (Holm et al., 1996) (Figure 1Ad). Adhesion was blocked by preincubation with F3 (Figure 1Aj), Notch1, or Notch2 antibodies (Figures 1Ae, 1Af, and 1Aj), but not with preimmune serum or antigen-depleted antibodies to Notch1 or Notch2 (Figures 1Ag, 1Ah, and 1Ai). We also used murine Notch1 (mN1)-transfected HeLa cells (Logeat et al., 1998) in cell repulsion assays (Figure 1B). mN1-transfected HeLa cells were repelled from F3 (Figure 1Ba) compared with mock-transfected HeLa cells (Figure 1Bb). Repulsion was reversed by pretreating the cells with F3 or Notch1 antibodies, but not with preimmune serum (Figure 1Bc). These studies suggest that Notch interacts with F3.

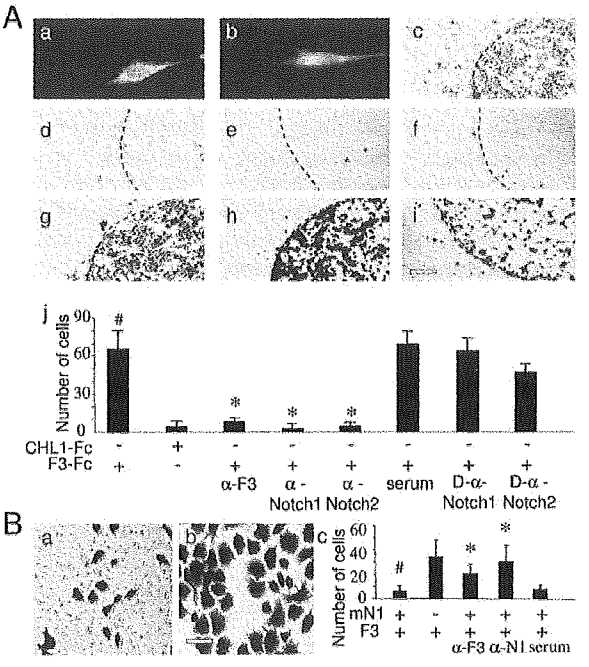

Figure 1. Notch and F3 Are Binding Partners

(A) Cell adhesion assay. OLN cells were labeled with α-Notch1 (a) or α-Notch2 (b). OLN cells were plated on dishes spotted with F3 (c and e–i) or CHL1 (d). Cells were untreated or pretreated prior to plating with α-Notch1 (e) or α-Notch2 (f), preimmune serum (serum) (g), or with antigen-depleted α-Notch1 (D-α-Notch1) (h) or α-Notch2 (D-α-Notch2) (i). Dotted lines depict the edges of the protein-Fc spots. Adherent cells were visualized by staining with Coomassie blue. (j) Quantification of OLN cell adherence to F3 substrate and the effects of blocking antibodies. #, $p < 0.05$ compared with CHL1; *, $p < 0.05$ compared with preimmune serum. Scale bar in (i): 20 μm for (a) and (b); 120 μm for (c)–(i).

(B) Cell repulsion assay. mN1- (a) or mock-transfected HeLa cells (b) were plated on F3-coated dishes. Adherent cells were stained with Coomassie Blue. (c) Quantification of HeLa cell adherence to F3 and the effects of blocking antibodies. In some experiments, mN1-transfected HeLa cells were pretreated with α-F3 or α-Notch1, or with preimmune serum (serum). #, $p < 0.05$ compared with mock-transfected HeLa cells; *, $p < 0.05$ compared with preimmune serum. Scale bar in (b): 15 μm for (a) and (b).

Bar graphs (Aj, Bc) represent the number of adherent cells (mean ± SD).

F3 Binds to Specific Sites on Notch1

To confirm F3/Notch interaction, rat brain membrane samples were immunoprecipitated with Notch1 or Notch2 antibodies. Immunoblotting of the precipitates using F3 antibody showed that they contained F3 (Figure 2Aa). In a reciprocal assay, an F3 antibody precipitate was probed with Notch1 or Notch2 antibodies (Figure 2Ab). These results indicate that Notch and F3 can form complexes.

To identify the specific binding site(s) on Notch1, we

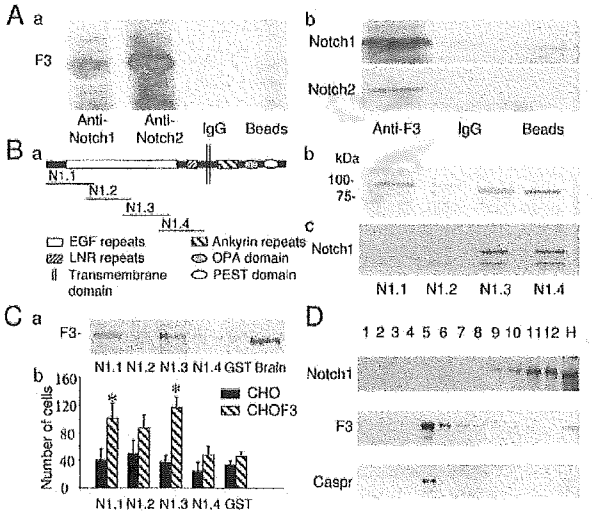

Figure 2. Notch and F3 Associate as a Protein Complex

(A) F3 coimmunoprecipitates with Notch1 or Notch2. (a) Immunoprecipitates from rat brain lysate were prepared using α-Notch1, α-Notch2, nonimmune IgG, or unconjugated beads, and were probed with α-F3. (b) Reciprocal assays used α-F3 to capture the protein complex, followed by immunoblotting with α-Notch1 or α-Notch2 to detect the binding partner.

(B) Subcloning of the Notch1 extracellular domain. (a) Schematic diagram of Notch1 and its subcloned fragments. (b and c) Coomassie Blue staining and α-Notch1 immunoblot of the four fragments, respectively.

(C) F3 binds to specific domains of Notch1. (a) The GST-Notch1 extracellular fragments (N1.1, N1.2, N1.3, and N1.4) or GST alone were used in a GST pull-down assay with rat brain lysate. The precipitates and rat brain lysate (right lane) were probed for F3. (b) Quantification of mock- and F3-transfected CHO cells adhering to culture dishes coated with the four GST fusion fragments or GST alone. Bars represent the number of adherent cells (mean ± SD). *, $p < 0.05$ compared with GST.

(D) Lipid raft analysis. F3 was mainly localized to the fifth fraction, while Notch1 was enriched in fractions 9–12. Caspr was used as a positive control to mark lipid raft fractions. H: Total homogenate.

divided the mouse Notch1 extracellular domain into four equal-sized fragments termed N1.1, N1.2, N1.3, and N1.4 (Figure 2Ba) and produced them as recombinant GST fusion proteins (Figures 2Bb and 2Bc). The Notch1 antibody used in the aforementioned cellular studies recognized only N1.3 and N1.4. GST pull-down assays with rat brain lysates revealed that F3 associated with N1.1 and N1.3 (Figure 2Ca). To confirm this, F3-transfected CHO cells (Gennarini et al., 1991) were seeded onto culture dishes coated with the four GST fusion proteins. Cells bound predominantly to N1.1 and N1.3. Mock-transfected CHO cells did not bind (Figure 2Cb).

F3 and Notch1 Are Not Colocalized in Lipid Rafts

F3 is a surface molecule localized in lipid rafts of OLs (Krämer et al., 1999). To ascertain whether F3/Notch interaction could occur in *cis* in these microdomains, they were isolated from P15 rat cerebral cortex. Both F3 and Caspr were detected in fraction 5 of the sucrose density gradient as reported (Faivre-Sarrailh et al., 2000), while Notch1 was found only in fractions 9–12 enriched in cytoskeleton-associated proteins (Figure 2D). The same results were obtained using adult rat cerebral cortex (not shown). Thus, F3 and Notch1 are unlikely to complex laterally within lipid rafts. Altogether, these observations suggest that F3 is a *trans* binding partner of Notch.

NICD Translocates to the Nucleus after Notch Interacts with F3

The immediate consequence of Notch activation is the release and transport of NICD to the nucleus (Schroeter et al., 1998). To determine if F3 could effect this, myc-tagged full-length mouse Notch1 (mNotch1-myc) was transfected into OLN cells. Cells were treated with different proteins and immunolabeled for NICD using NICD antibody (Logeat et al., 1998). In F3-treated cells, concentrated NICD staining was observed in the nuclei (Figure 3Aa), similar to Jagged1-induced NICD translocation (Figure 3Ab). BSA failed to trigger this event (Figure 3Ac). Preincubation with Notch1 EGF antibody (which cross-reacts with Notch2, not shown) abolished F3-induced NICD translocation (Figure 3Ad). Brefeldin A and monensin (not shown), compounds that inhibit the membrane insertion of Notch1 (Schroeter et al., 1998), also prevented NICD translocation. Cell treatment with increasing concentrations of F3 or Jagged1 led to a similar concentration-dependent increase in nuclear clustering of NICD (Figure 3Ae). OLN cocultured with either F3- or Jagged1- but not mock-transfected CHO cells also resulted in production of Notch2 intracellular domain (ICD) (Figure 3Af). Notch2 ICD antibody was not cross-reactive with Notch1 ICD (not shown). These results demonstrate that F3, like Jagged1, can activate Notch1 and Notch2, leading to subsequent nuclear translocation of NICD.

F3 Induces Notch Intramembrane Cleavage at the S3 Site

As a prerequisite for activation, Notch undergoes γ-secretase-dependent RIP at the S3 site (V1744) (Schroeter et al., 1998; Huppert et al., 2000). To clarify the nature of F3-induced cleavage, mNotch1-myc transfected OLN cells were preincubated with γ-secretase inhibitor and then treated with F3 or Jagged1. In both cases, no NICD staining was observed in the nuclei (Figures 3Ba and 3Bb). Moreover, two S3 cleavage mutants, V1744K-myc and V1744L-myc, which showed reduced proteolysis and parallel reduction in activity (Schroeter et al., 1998), were transfected into OLN cells that were then treated with F3 or Jagged1. Cells showed c-*myc* immunostaining mainly in the cytoplasm and on the cell surface, but not in the nuclei (Figures 3Bc–3Bf). In immunoprecipitation assays, c-*myc* antibody precipitates from F3- or Jagged1-treated V1744K-myc and V1744L-myc transfected OLN cells could only be labeled with NICD antibody that also recognizes full-length Notch1 (300 kDa) (Figure 3Bg, upper panel), indicating that these mutant Notch1 molecules remained intact. Only the precipitates from F3- or Jagged1-treated mNotch1-myc transfected OLN cells showed a reactive band upon probing with V1744 antibody that solely recognizes NICD released from S3 (120 kDa) (Figure 3Bg, lower panel). Altogether, these observations suggest that F3 induces RIP at the Notch1 S3 site.

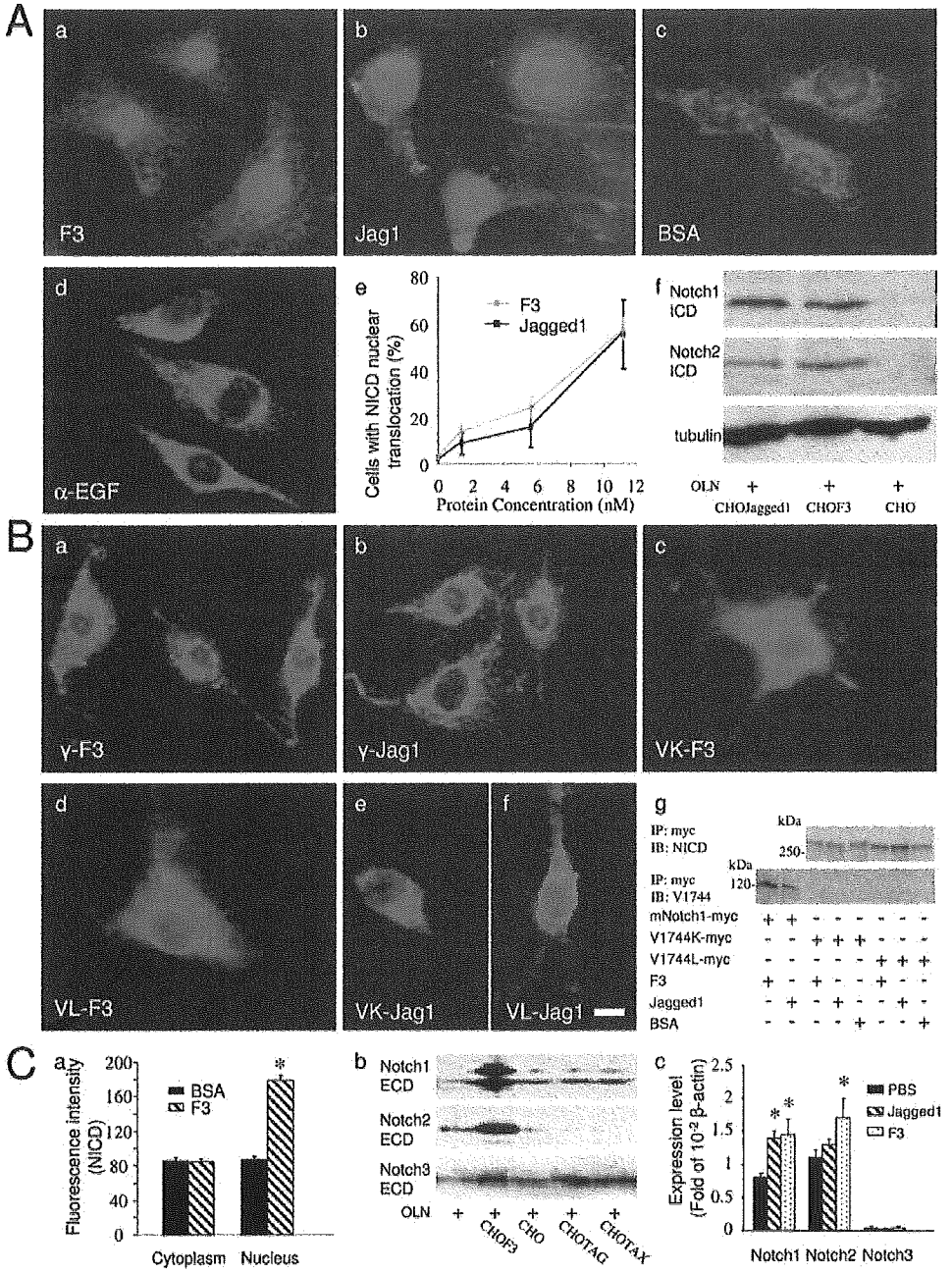

Figure 3. NICD Translocation

(A) F3-induced NICD nuclear translocation. mNotch1-myc transfected OLN cells were treated with 11.2 nM F3 (a), Jagged1 (b), BSA (c), or preincubated with α-Notch1 EGF prior to F3 treatment (d) and then stained with α-NICD. (e) Quantification of cells with nuclear staining of NICD after treatment with increasing concentrations of F3 and Jagged1. Data are mean ± SEM. (f) OLN cells were cultured with Jagged1-, F3-, or mock-transfected CHO cells, and lysates were immunoprobed with α-Notch1, α-Notch2, and α-tubulin.

(B) F3-induced RIP involves γ-secretase at the S3 site. OLN cells were pretreated with 200 μM γ-secretase inhibitor, stimulated with F3 (a) or Jagged1 (b), and stained with α-NICD. After treatment with F3 (c and d) or Jagged1 (e and f), myc-tagged V1744K or V1744L mutant-transfected OLN cells were immunolabeled for c-*myc*. (g) α-c-*myc* immunoprecipitates from OLN cells expressing myc-tagged wild-type Notch1 or V1744K and V1744L mutants were immunoblotted with α-NICD (which recognizes both the ~300 kDa full-length and the ~120 kDa intracellular portion of Notch1) or α-V1744 (which only recognizes NICD after cleavage at the S3 site). Scale bar in (Bf): 15 μm for (Aa)–(Ad) and (Ba)–(Bf).

(C) Upregulation of Notch1 and Notch2. Total (cytoplasmic plus nuclear) NICD staining intensity was quantified in F3-treated and BSA-treated mNotch1-myc transfected OLN cells (a). OLN cells cultured alone or with F3-, mock, TAG-1-, or TAX-transfected CHO cells were lysed and probed with α-Notch1, α-Notch2, and α-Notch3 (b). (c) Real-time PCR assays of Notch mRNA levels in OLN cells treated with 11.2 nM F3, Jagged1, or PBS. Raw data were normalized to β-actin. Bars are mean ± SEM. *, $p < 0.05$ compared with PBS.

F3/Notch Interaction Upregulates Notch1 and Notch2 Expression

F3, but not BSA, induced a 2-fold increase in nuclear NICD (Figure 3Ca), while there was no noticeable change in cytoplasmic NICD, suggesting that F3 upregulates Notch expression. To confirm this, OLN cells were cultured with mock-, F3-, TAG-1-, or TAX-transfected CHO cells. TAG-1 and TAX are members of F3 subfamily (Tsiotra et al., 1993). Expression of Notch1 and Notch2, but not Notch3, increased when OLN cells were cultured with F3-transfected CHO cells (Figure 3Cb). Real-time PCR showed that soluble F3 increased Notch1 and Notch2, but not Notch3 transcripts (Figure 3Cc), while Jagged1 only upregulated Notch1, but not Notch2. Thus, F3/Notch interaction may provide a feedback loop to specifically upregulate Notch1 and Notch2.

Oligodendroglial Processes Alter their Morphology upon Contact with F3

To model the scenario of axoglial contact during myelination, we studied the morphology of OLN processes when they contact cell surface-expressed F3. Since OLN cells extend longer processes than primary OLs, they are ideally suited for observing subtle morphological changes that occur during contact. F3-transfected CHO cells mimicked the paranodal axonal component. Mock-, TAG-1-, and TAX-transfected CHO cells were used as controls. Remarkably, most OLN processes terminated upon contact with F3-transfected CHO cells and flattened to form a cytoplasmic sheet spreading over the surface of CHO cells, as if in an attempt to envelop the cell (Figures 4A–4K). But this was not observed with mock- (Figures 4L and 4M), TAG-1- (Figures 4N and 4O), or TAX-transfected (Figures 4P and 4Q) CHO cells. While approximately 80% of extending processes halted upon reaching F3-transfected CHO cells, with other CHO cells the proportion was only 20% (Figure 4R). These results suggest that a signal inducing the morphological change is presented to the oligodendroglial processes when F3 is encountered.

F3, but Not Jagged1, Upregulates MAG

To explore how the morphological change described above could relate to F3/Notch signaling, we investigated the expression of myelin-associated glycoprotein (MAG), a mature OL marker, in the aforementioned cocultures. Parental and transfected CHO cells did not express Delta, Jagged1, and Jagged2 (Figure 5Aa). Membrane extracts of cocultured cells were immunoblotted for MAG. The constitutive level of MAG in OLN cells was very low, if not undetectable. However, when OLN cells were cultured with F3-transfected CHO cells, MAG was upregulated (Figure 5Ab). F3-transfected CHO cells do not express MAG (not shown). In real-time PCR, primary OLs plated upon F3 substrate showed approximately sixteen-fold increase in MAG transcripts versus cells seeded on BSA (Figure 5Ac). OLN cells showed a similar efficiency of MAG upregulation (not shown).

Furthermore, mNotch1-myc transfected OLN cells were immunolabeled for MAG and 2′, 3′-cyclic nucleotide 3′-phosphodiesterase (CNPase), an OL-specific antigen. Treatment with soluble F3 resulted in a remarkable increase in MAG staining (Figure 5Ba) and enhanced CNPase staining (Figure 5Bd), compared with Jagged1 (Figures 5Bb, 5Bc, 5Be, and 5Bf) or BSA (not shown) treatment. Quantification of MAG and CNPase fluorescence intensities revealed an approximately 300% increase in MAG and 40% increase in CNPase labeling in F3- versus Jagged1- or BSA-treated cells (Figure 5Bg). Cell pretreatment with Notch1 EGF antibody prevented F3-induced increase in MAG and CNPase (Figure 5Bg), suggesting that Notch is required for this event. In addition, F3 induced cells to flatten and form a sheet-like structure (Figure 5Ba). Quantification of the substratum area covered by cells revealed a 2-fold increase in that covered by F3-versus Jagged1- or BSA-treated cells (Figure 5Bh). These findings confirm F3-induced MAG upregulation.

MAG Is Upregulated by F3/Notch Interaction

To better understand the involvement of NICD in this event, we transiently transfected into OLN cells V5-tagged dominant-negative Notch1 (dn-N1) or Notch2 (dn-N2) (Small et al., 2001), which lack the intracellular regions but can bind to extracellular ligands. Cells were then treated with F3 and double stained with V5 and MAG antibodies. Notably, both dn-N1-V5- (Figure 5Ca) and dn-N2-V5- (Figure 5Cb) positive cells were poorly labeled for MAG. pcDNA4/V5/LacZ (LacZ) was used as a vector control (Figure 5Cc). Moreover, OLN cells transfected with myc-tagged V1744K (Figure 5Cd) and V1744L (Figure 5Ce) were treated with F3 and double stained for c-*myc* and MAG. In either case, F3 failed to upregulate MAG in c-*myc*-positive cells. Quantification of MAG fluorescence intensity confirmed that Notch1 or Notch2 dysfunction, in other words, the absence of NICD, abolished F3-induced MAG upregulation (Figure 5Cj), suggesting that NICD is required for MAG expression.

We further investigated the inductive role of F3 in this event by introducing into OLN cells V5-tagged constitutive-active Notch1 (caN1) (Figures 5Cf and 5Cg) and Notch2 (caN2) (Figures 5Ch and 5Ci), which lack the extracellular domains and are ligand-independently active (Small et al., 2001). That is, even in the absence of F3, NICD is generated and translocates to the nucleus. In OLN cells, caN1 (Figure 6Ac) and caN2 (not shown) transactivated Hes1 in luciferase reporter assays. Immunolabeling showed that V5-positive cells were faintly stained for MAG (Figure 5Cj). Given that Jagged1 also induces NICD release, but does not increase MAG expression, these results demonstrate that MAG upregulation requires F3-induced NICD.

F3/Notch-Induced MAG Upregulation Is Independent of *Hes1*

A prominent feature of Notch signaling is the expression of *Hes* genes in an oscillatory manner (Hirata et al., 2002). We thus quantified *Hes1* mRNA levels in OLN cells using real-time PCR. Nonphysiological treatment of cells with 2 mM EDTA (Rand et al., 2000) triggered a sharp increase in *Hes1* mRNA during the first two hours and a return to basal level by three hours (Figure 6Aa), reflecting the exquisite regulation of endogenous *Hes1* expression (Dale and Maroto, 2003). However, F3, Jagged1, or BSA treatment did not significantly alter the baseline oscillating levels of endogenous *Hes1* tran-

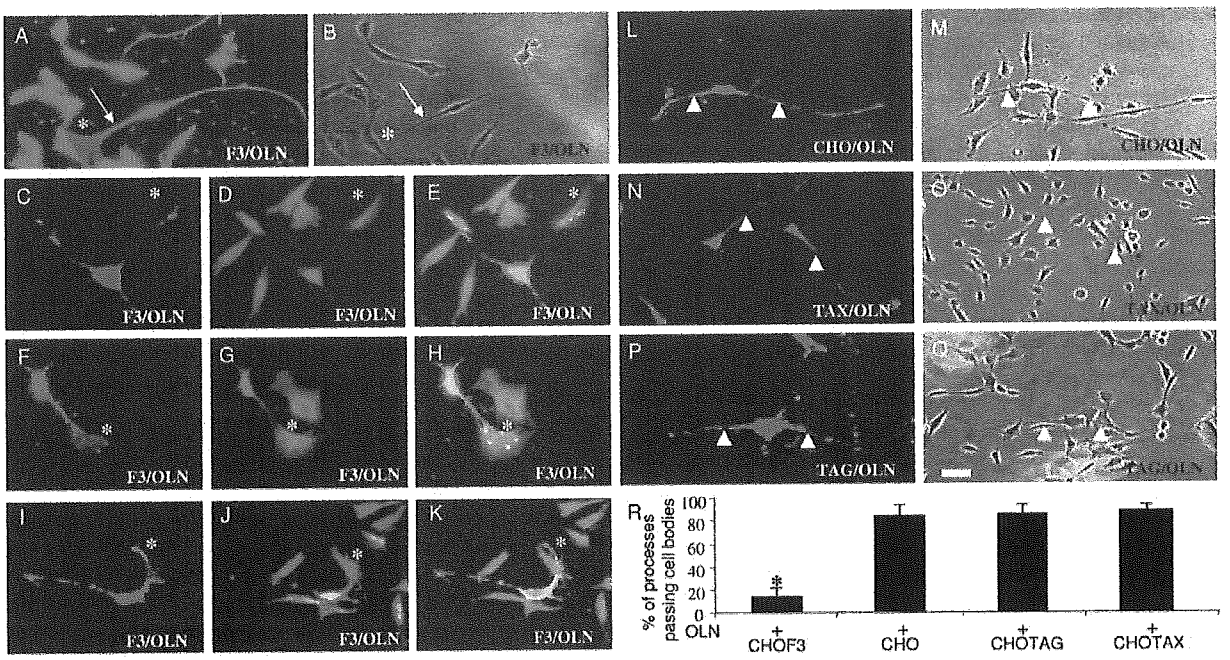

Figure 4. OLN Cellular Processes Halt and Alter their Morphology upon Contact with F3-Transfected CHO Cells

Cellular processes (arrows in [A] and [B]) of OLN cells extend toward F3-transfected CHO cell somata and upon contact with them, terminate and elaborate a flattened cytoplasmic sheet that envelops the cell body. This phenomenon is indicated by asterisks (*).

(A) Both OLN and F3-transfected CHO cells were prestained with PKH26 red fluorescent dye.

(B) The bright-field micrograph corresponding to (A).

(C, F and I) OLN cells were prestained with PKH26 red fluorescent dye.

(D, G, and J) Both OLN cells and F3-transfected CHO cells were stained for c-*myc* (green).

(E, H, and K) Merged images of (C) and (D), (F) and (G), and (I) and (J), respectively.

(L–Q) In the control systems, cellular processes (arrowheads) of OLN cells extend past transfected CHO cell bodies. (L) and (M), (N) and (O), and (P) and (Q) are corresponding PKH26 red fluorescent and bright-field micrographs of cocultures of OLN cells with mock- (L and M), TAX- (N and O) and TAG-1- (P and Q) transfected CHO cells.

(R) Quantification of OLN cellular processes extending past transfected CHO cell bodies in the cocultures. Data are mean ± SD. *, $p < 0.01$ compared with controls. Scale bar in (Q): 25 μm for (A), (B), and (L–Q) and 15 μm for (C)–(K).

scription at short (the first three hours) or long (12 and 24 hr) times after treatment (Figure 6Aa).

To investigate whether F3-induced MAG upregulation relates to constitutive level of *Hes1* protein, *Hes1* antisense oligonucleotides (Kabos et al., 2002) were used to block basal *Hes1* protein expression in OLN cells (Figure 6Ab). MAG upregulation was not influenced by this treatment or control sense oligonucleotides (Figures 6Ad, 6Ae, and 6Ag).

Furthermore, we transfected OLN cells with dominant-negative RBP-J-myc (dn-RBP-J-myc), bearing a mutation of lysine 218 to histidine, which abolishes effective high affinity binding to *Hes1* promoter region (Kato et al., 1997). Hes1 luciferase reporter assay showed that the mutant prevented *Hes1* activation by caN1 (Figure 6Ac). After transfection, cells were treated with F3 and double labeled for c-*myc* and MAG. c-*myc* positive cells showed the same level of MAG as neighboring nontransfected cells (Figures 6Af and 6Ag). These results indicate that MAG upregulation triggered by F3/Notch signaling is independent of endogenous *Hes1* expression.

F3/Notch-Induced MAG Upregulation Involves DTX1

Given that F3-induced MAG upregulation does not involve *Hes1*, we investigated the role of another Notch downstream element, DTX1, in this event using myc-tagged wild-type DTX1 (Yamamoto et al., 2001) and its two deletion mutants, HA-tagged DTX1 mutant (DTX1-D1), containing amino acids 1–411 (Yamamoto et al., 2001), and Flag-tagged DTX1 mutant (DTX1-D2), containing amino acids 1–242 (Izon et al., 2002) (Figure 6Ba). The two mutants lack the Ring-H2 finger motif, which contributes to DTX1 oligomerization, an essential step for DTX1 functioning (Matsuno et al., 2002). As previously observed (Yamamoto et al., 2001), Hes1 luciferase reporter assay showed that overexpressed DTX1 inhibited the transactivation of *Hes1* by caN1 (Figure 6Bb), while both DTX1-D1 and DTX1-D2 restored *Hes1* response to caN1 (Figure 6Bb). After transfection, OLN cells were treated with F3 and double labeled for MAG and corresponding tags. Overexpression of DTX1 had no effect on F3-induced MAG upregulation (Figures 6Bc–6Be and 6Bl). Interestingly, MAG upregulation was abolished in the HA-positive or Flag-positive cells (Figures 6Bf–6Bl). These observations strongly suggest that F3/Notch-induced MAG upregulation involves DTX1.

F3/Notch Signaling Pathway via DTX1 Promotes OPC Differentiation into OLs

The Jagged1/Notch signaling pathway inhibits OPC differentiation into OLs (Wang et al., 1998). To explore

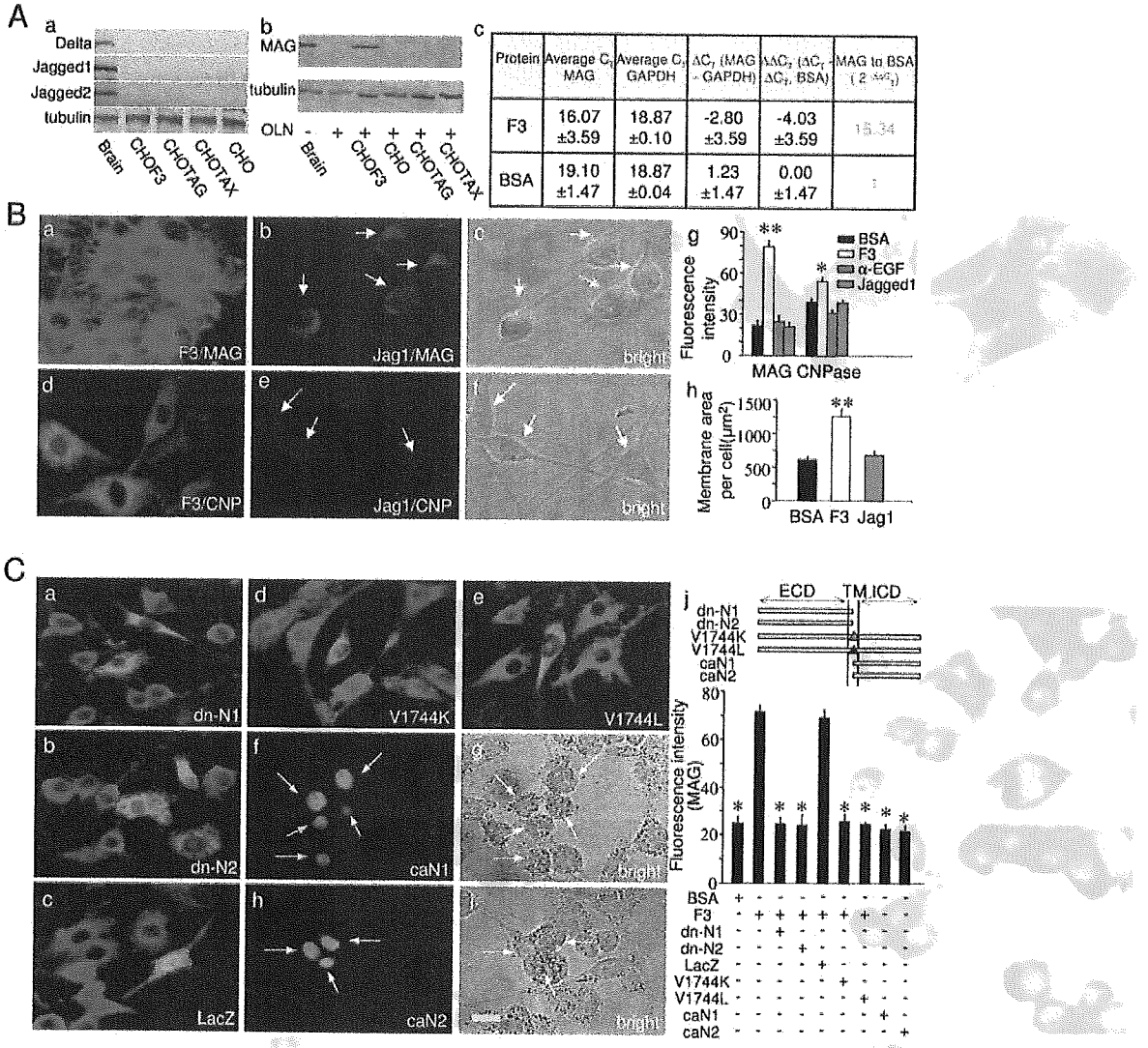

Protein	Average C_T MAG	Average C_T GAPDH	ΔC_T (MAG - GAPDH)	$\Delta\Delta C_T$ (ΔC_T - ΔC_T, BSA)	MAG to BSA ($2^{-\Delta\Delta C_T}$)
F3	16.07 ±3.59	18.87 ±0.10	-2.80 ±3.59	-4.03 ±3.59	16.34
BSA	19.10 ±1.47	18.87 ±0.04	1.23 ±1.47	0.00 ±1.47	1

Figure 5. MAG Is Upregulated by F3/Notch Interaction

(A) MAG is upregulated by F3. CHO cells and transfected derivatives do not express classic ligands of Notch, Delta, Jagged1, and Jagged2 (a). Lysates of rat brain, OLN alone and the indicated cocultured cells were probed with α-MAG (upper panel) or α-γ-tubulin (bottom panel) (b). (c) Measured by real-time PCR, MAG mRNA in primary OLs is elevated significantly by F3 versus BSA treatment. The raw data were normalized to GAPDH using comparative C_T method.

(B) F3, but not Jagged1, upregulates MAG. mNotch1-myc transfected OLN cells were treated with 11.2 nM F3-Fc (a and d) or Jagged1 (b, c, e, and f) and labeled using α-MAG (a and b) or α-CNPase (d and e). The arrows in (b) and (e) indicate the cell bodies, which can be better viewed in bright-field pictures (c and f). (g) Fluorescence intensities of MAG and CNPase staining in cells treated with F3, Jagged1, or BSA, or pretreated with α-Notch1 EGF followed by F3. Data are mean ± SEM. (h) Quantification of the surface area (mean ± SEM) occupied by cells treated with F3, Jagged1, or BSA. *, $p < 0.05$; **, $p < 0.01$ compared with BSA.

(C) MAG upregulation is F3/Notch interaction-dependent. OLN cells transfected with Notch ICD-deleted mutants dn-N1 (a) and dn-N2 (b); LacZ (c); S3 cleavage mutants V1744K (d) and V1744L (e); or Notch ECD-deleted mutants caN1 (f and g) and caN2 (h and i). The cells were then treated (a–e) or untreated (f–i) with 11.2 nM F3 and double labeled for MAG (red) and V5 (a–c, f, and h) (green) or c-myc (d and e) (green). The transfected cells in (f) and (h) can be better viewed as indicated by arrows in bright-field pictures (g) and (i), respectively. (j) MAG fluorescence intensities in cells transfected with various indicated constructs followed by different protein treatments. Data are mean ± SEM. ECD, extracellular domain; TM, transmembrane domain; ICD, intracellular domain. The S3 site mutations in V1744K and V1744L constructs are indicated by triangles in the transmembrane region. *, $p < 0.01$ compared with F3-treated OLN cells. Scale bar in (Ci): 20 μm for (Ba)–(Bf); 40 μm for (Ca)–(Ci).

whether F3/Notch signaling via DTX1 instructs OPC differentiation, purified OPCs positive for the progenitor marker Ng2 (Dawson et al., 2000) (Figure 7Aa) were treated with BSA, F3, or Jagged1 for 2 days and then double stained for Ng2 and CNPase (Figures 7Ab–7Ad). After F3 treatment, over 70% of OPCs differentiated into CNPase+ OLs compared to ~50% after BSA stimulation, while Jagged1 treatment resulted in nearly all OPCs remaining undifferentiated (Figure 7Ak). F3-stimulated cells were more bifurcated and inclined to form a web-like structure (Figure 7Ac) than BSA-treated cells (Figure 7Ab). Notch and DTX1 involvement was examined by transfecting

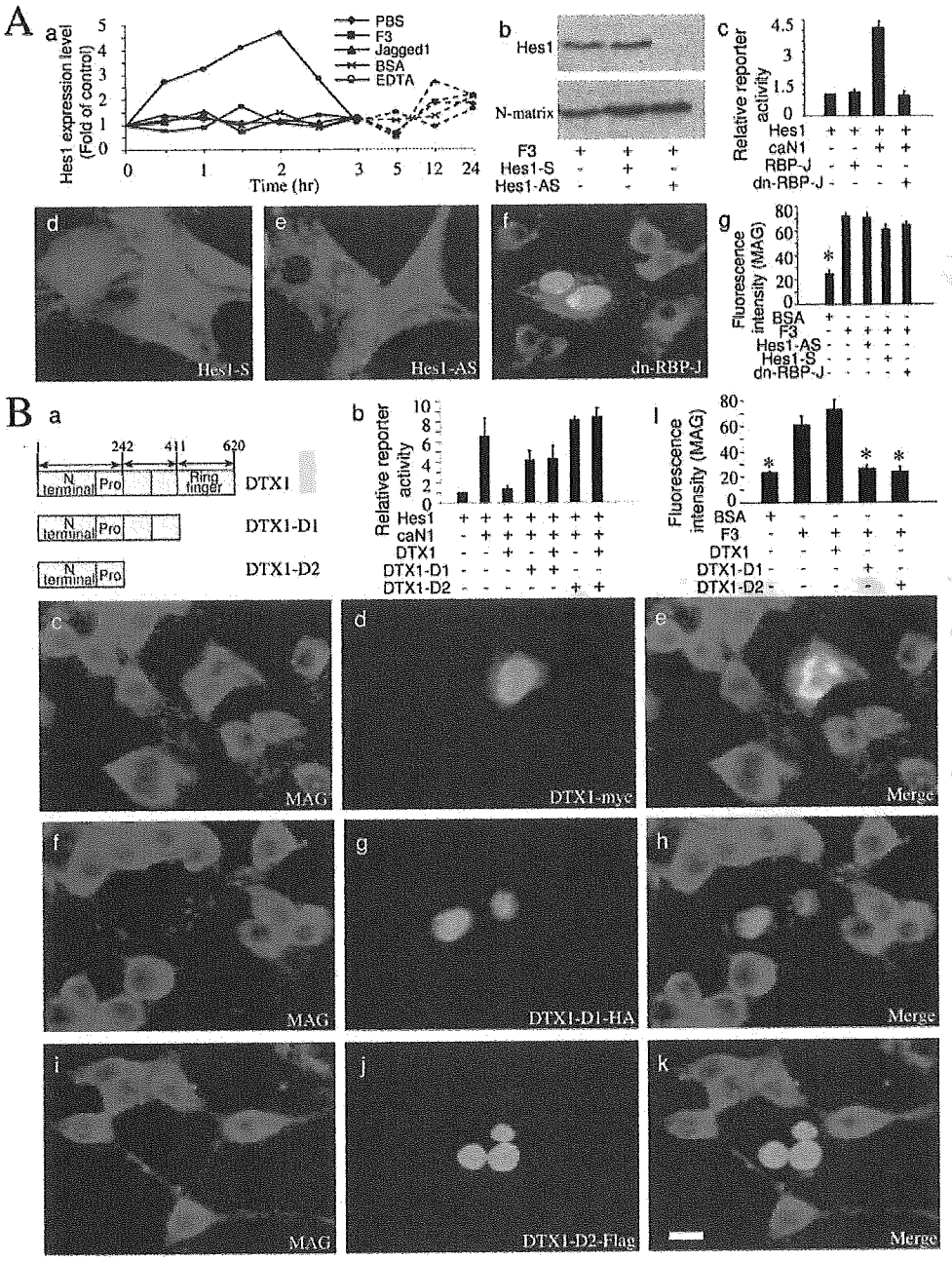

Figure 6. MAG Expression Is Independent of *Hes1* and Dependent on DTX1

(A) MAG upregulation is independent of *Hes1* expression. (a) OLN cells were treated with the indicated ligands or compounds. At the times shown, *Hes1* transcripts were quantified using real-time PCR and normalized to that at the start of the time course. (b, d, and e) OLN cells were untreated or pretreated with *Hes1* sense (Hes1-S) or antisense (Hes1-AS) oligonucleotides followed by 11.2 nM F3. Cell lysates were probed with α-Hes1 (upper panel) or α-nuclear matrix protein (N-matrix) (bottom panel) (b) or cells were labeled for MAG (d and e). Also, OLN cells transfected with pGVB/Hes1 reporter alone or together with constructs expressing caN1, RBP-J, or myc-tagged dn-RBP-J were subjected to luciferase assay (c). Data are mean ± SD. (f) OLN cells transfected with dn-RBP-J-myc were treated with 11.2 nM F3 and double stained for MAG (red) and c-*myc* (green). (g) MAG staining intensity in OLN cells with various treatments indicated above. Data are mean ± SEM. *, $p < 0.01$ compared with cells treated with F3 alone.

(B) MAG upregulation involves DTX1. (a) DTX1 constructs used in luciferase reporter assays and immunostaining study. N-terminal, N-terminal domain; Pro, proline-rich motif; Ring finger, Ring-H2 finger motif. OLN cells were transfected with pGVB/Hes1 reporter alone or together with indicated expression constructs. (b) Luciferase reporter activity in these cells. Data are mean ± SD. DTX1- (c–e), DTX1-D1-HA- (f–h), or DTX1-D2-Flag- (i–k) transfected OLN cells were treated with 11.2 nM F3 and double labeled for MAG (red) and related tags (green). (l) MAG fluorescence intensity in OLN cells transfected with indicated constructs followed by different protein treatments. Data are mean ± SEM. *, $p < 0.01$ compared with F3-treated OLN cells. Scale bar in (Bk): 30 μm for (Ac)–(Af) and (Bc)–(Bk).

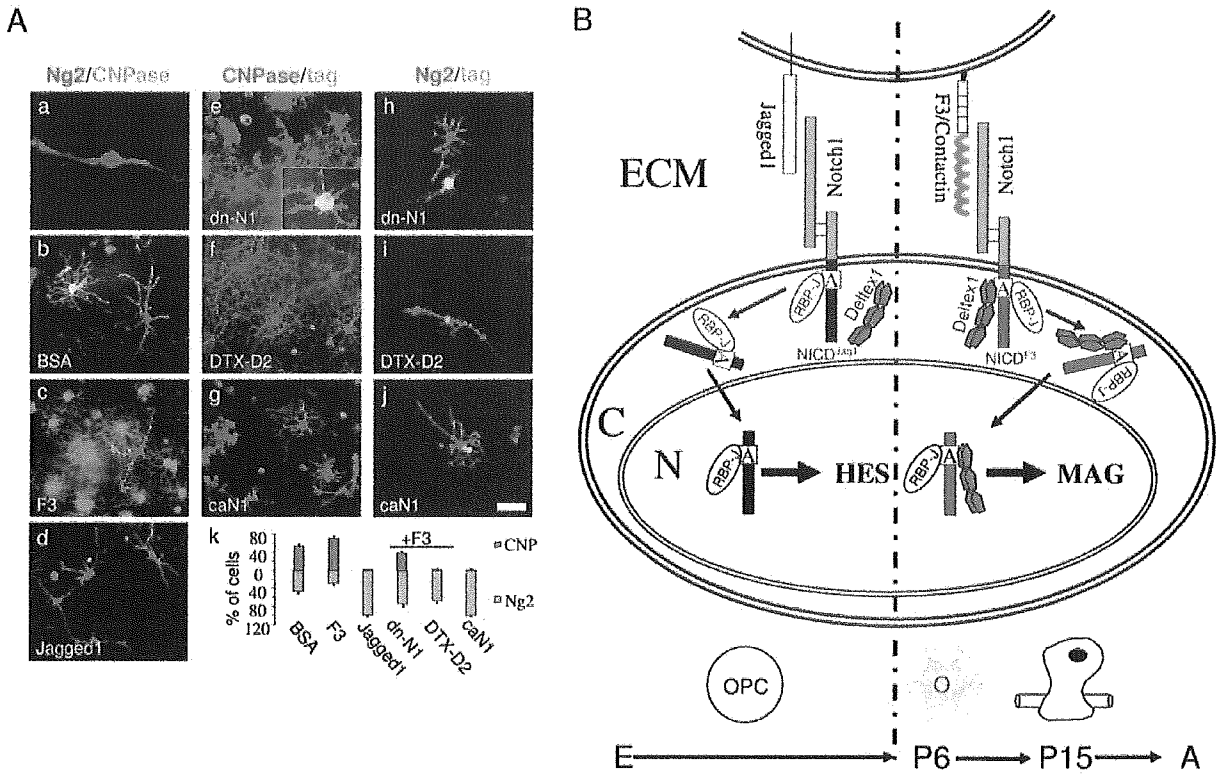

Figure 7. F3/Notch Interaction Induces OPC Differentiation

(A) F3/Notch signaling via DTX1 promotes OPC differentiation. Purified Ng2+/CNPase-OPCs (a) were treated with BSA (b), F3 (c), or Jagged1 (d) for 2 days, double labeled for Ng2 (red) and CNPase (green), and counted (k). Some OPCs were transfected with tagged dn-N1 (e and h) and DTX1-D2 (f and i) followed by F3 treatment. Other OPCs were transfected with caN1 and left untreated (g and j). Cells were double stained for the appropriate tag (green) and CNPase (red; e–g) or Ng2 (red; h–j) and counted (k). Scale bar in (j): 25 μm for (a) and (e, inset), 100 μm for (b)–(j).

(B) Proposed model of ligand-dependent Notch signaling pathways during development. F3 interacts with the Notch receptor on the opposing cell surface to stimulate Notch/RBP-J signaling pathway to recruit DTX1 before or after releasing NICD into the cytoplasm. The NICD/RBP-J/DTX1 complex may undergo specific but unidentified modification prior to translocation into the nucleus, where it activates target genes such as MAG. This signaling may contribute to OL maturation after P6, when decreased Jagged1 expression favors the initiation of F3/Notch signaling. In contrast, before P6, Jagged1/Notch signaling activates the NICD/RBP-J-dependent transcription of target genes such as *Hes1* and predominantly inhibits OPC differentiation. ECM, extracellular matrix; C, cytoplasm; N, nucleus; $NICD^{Jag1}$ and $NICD^{F3}$, NICD released upon Jagged1 and F3 activation, respectively; E, embryo; P6 and P15, postnatal day 6 and 15, respectively; A, adult; O, oligodendrocyte; right bottom cartoon: myelinating oligodendrocyte ensheathing the axon.

OPCs with dn-N1-V5 (Figures 7Ae and 7Ah) and DTX1-D2-Flag (Figures 7Af and 7Ai), respectively, followed by F3 treatment for 2 days. Other OPCs were transfected with caN1-V5 and left untreated (Figures 7Ag and 7Aj). Notably, immunolabeling for tags and CNPase (Figures 7Ae–7Ag) or Ng2 (Figures 7Ah–7Aj) showed that most dn-N1 (~75%) or DTX1-D2 (~67%) transfected OPCs remained Ng2+ (Figure 7Ak), despite the presence of F3. In particular, ~40% of dn-N1-transfected cells were CNPase+, but these cells were less bifurcated (Figure 7Ae, inset), compared to surrounding nontransfected cells, indicating a relatively immature stage. However, CNPase+ DTX-D2-transfected cells were hardly detectable. Consistent with a previous report (Wang et al., 1998), caN1-transfected cells remained Ng2+, and almost none became CNPase+ OLs (Figure 7Ak), indicating that F3-induced NICD is specifically required for accelerated OPC differentiation. These results demonstrate that F3/Notch signaling via DTX1 promotes OPC development.

Discussion

Our data designate the adhesion molecule F3 as a functional ligand of Notch. F3/Notch interaction induces the generation and nuclear translocation of NICD and elevates Notch1 and Notch2 expression. It promotes OPC differentiation and upregulates MAG in OLN cells and primary OLs, revealing a potential regulatory role for F3 in OL development. Thus, ligand-specific Notch signaling via Jagged1 as an inhibitory factor and F3 as a positive instructor may coordinate myelination (Figure 7B).

Notch Is an Oligodendroglial Surface Receptor of F3

Adhesive contacts at axoglial junctions are partly contributed by the F3-Caspr-neurofascin 155 heterotrimer (Girault and Peles, 2002). Herein we define a functional ligand-receptor interaction between F3 and Notch. Cell adhesion/repulsion assays and biochemical approaches demonstrate that Notch and F3 are binding partners.

Further, we have identified two extracellular sites on Notch1 for F3 binding, namely N1.1 and N1.3. The former contains the EGF repeats 11–12 involved in DSL binding (Rebay et al., 1991). F3 is also expressed on OLs (Koch et al., 1997) and transduces signals to glial intracellular Fyn, which then interacts with Tau protein to mediate myelination (Klein et al., 2002). Since soluble F3 is sufficient to trigger F3/Notch signaling and the lipid raft assay demonstrated that Notch1 is not localized to the F3-enriched fraction, F3 may not interact with Notch1 in *cis*. Given that Notch and F3 colocalize in various regions of the brain (Lardelli et al., 1994; Revest et al., 1999), particularly at axoglial junctions, our results suggest a role for F3 as a *trans*-acting ligand of Notch.

F3/Notch Signaling Induces Proteolytic Release of NICD and Upregulates Notch Homologs

RIP, the generation of nuclear signaling proteins derived from nonnuclear precursors such as Notch and APP, is a new paradigm of signal transduction that adds unforeseen diversity to the signaling repertoire of a cell (Ebinu and Yankner, 2002). We have shown that F3 binding triggers Notch intramembrane proteolysis at the S3 site and nuclear translocation of the resultant NICD in OLN cells. The ability of Notch1 EGF antibody or brefeldin A and monensin to block this event suggests that the extracellular F3/Notch interaction is essential for the intramembrane cleavage-derived generation and transport of NICD. Thus, it is another example of RIP. In addition, the F3/Notch signaling pathway may specifically increase Notch1 and Notch2 (but not Notch3) expression or protect Notch1 and Notch2 from rapid degradation. Either way, this may serve to replenish consumed receptors on the cell surface and thus sustain signal continuity.

A Possible Model for F3/Notch Signaling via DTX1

Given that F3 and Jagged1 share a common binding domain on Notch1, Jagged1 downregulation that occurs prior to myelination may permit the alternate interaction of Notch with F3. In OLN cells, both Jagged1 and F3 trigger γ-secretase-mediated and S3-directed release of NICD followed by its nuclear translocation. Moreover, caN1 activates *Hes1*, which is blocked by coexpression of dn-RBP-J-myc or DTX1. Thus, it is conceivable that F3-induced Notch intracellular signaling is associated with RBP-J. However, only F3-induced NICD, but not Jagged1-induced NICD or caN1 or caN2, induces OPC differentiation and increases MAG expression, suggesting that this event may require specific extracellular ligand-receptor interaction. Moreover, experiments utilizing either dn-RBP-J-myc or *Hes1* antisense oligonucleotides indicate that the blockage of endogenous *Hes1* expression is not involved in F3/Notch-induced MAG upregulation. On the other hand, two truncated mutants of DTX1, which lack the Ring-H2 finger motif that is indispensable for the formation of functional homodimeric DTX1 (Matsuno et al., 2002), prevent both F3-promoted OPC differentiation and MAG upregulation. Thus, we propose that a switch in ligands may alter Notch intracellular signaling effectors (Figure 7B). The binding of different ligands may induce the formation of distinct Notch conformations. Such conformational alterations could result from different, albeit overlapping, regions of Notch recognized by Jagged1 and F3. Notch receptors with distinct conformations may interact, before or after cleavage, with different cytoplasmic factors, such as DTX1. The form of NICD subsequently arriving at the nucleus then specifies further potential interactions and determines its transcriptional target. It will be of significance to investigate this hypothesis and identify DTX1-related transcription cofactors that are required for F3/Notch signaling.

Potential Role of F3/Notch Signaling via DTX1 in OL Maturation

Jagged1/Notch signaling contributes to maintaining OPCs in an undifferentiated stage (Wang et al., 1998). The failure of efficient remyelination in multiple sclerosis (MS) has been partly attributed to the activation of OPC Notch by astrocyte-expressed Jagged1 (John et al., 2002). However, Jagged1 expression sharply decreases from around P6 (Wang et al., 1998), a time point concurrent with the onset of myelination and the clustering of axonal F3 at the paranode (Kazarinova-Noyes et al., 2001), an ideal position to interact with Notch receptors on the surface of newly formed OLs. Mutant animals, in which Notch1 is selectively ablated in OPCs (Genoud et al., 2002), are characterized by ectopic immature OLs, most of which undergo apoptosis, indicating that autonomous differentiation in the absence of the Notch receptor may be disruptive and that other regulatory signaling cascades besides Jagged1/Notch may be needed to ensure correct differentiation and survival of OLs. We observed here that F3 promotes OPC differentiation, which can be blocked by both dominant-negative Notch and DTX1 deletion mutants, and oligodendroglial processes emanating from OLN cells terminate and spread over the surface of F3-transfected CHO cells, an event related to the upregulation of myelin-specific proteins, such as MAG and CNPase. Upon Notch interaction with either immobilized or soluble F3, MAG is significantly upregulated at both the protein and mRNA levels. MAG upregulation can be blocked by dominant-negative construct of Notch1, Notch2, or deletion mutants of DTX1. These observations indicate that OL maturation involves F3/Notch signaling via DTX1 (Figure 7B).

In summary, our study reveals a new facet of the Notch signaling pathway. Upon activation by F3, Notch signaling via DTX1 continues to participate in OL maturation through upregulating certain myelin-related proteins instead of solely functioning to inhibit OPC differentiation into OLs. Hence, this finding may prove to be an efficient molecular handle for promoting remyelination in degenerative diseases, such as MS, by creating an environment in which Notch predominantly interacts with endogenous or exogenous F3 to initiate the F3/Notch/DTX1 signaling pathway.

Experimental Procedures

Antibodies

The following antibodies were used: Monoclonal Notch1 EGF (Neomarker), CNPase and Flag (Sigma), c-*myc* (9E10) and HA (Santa Cruz Biotechnology), nuclear matrix (Chemicon) and V5 (Invitrogen) antibodies, polyclonal V1744 (Cell Signaling), N2ICD, Jagged1, Jagged2, Delta (Santa Cruz Biotechnology), γ-tubulin (Sigma), Ng2

(Chemicon), Hes1 (Kaneta et al., 2000), NICD (Logeat et al., 1998), Notch1, Notch2, Notch3 (kind gifts from Dr. Lendahl), and F3 (Shimazaki et al., 1998). Polyclonal Caspr antibody was obtained by immunization of rabbits with a GST fusion protein of amino acids 277–430 of human Caspr and polyclonal MAG antibody (7610) with the following peptide: N′-CISCGAPDKYESREVST-C′ (Eurogentec).

Cell Adhesion/Repulsion Assay

Cell adhesion/repulsion assay was performed as described (Xiao et al., 1996).

Fusion Proteins

Production of F3-Fc Fusion Proteins

Recombinant cDNA encoding mouse F3 with the GPI-anchor substituted with human IgG Fc was inserted at the Hind III-Not I sites of pDX with an amplification-promoting sequence (APS) (Hemann et al., 1994) and introduced into $Ltk^{-/-}$ cells. Fc fusion proteins were purified as described (Shimizu et al., 1999).

Production of Notch1-GST Fusion Proteins

The following regions of the mouse Notch1 extracellular domain were subcloned into pGEX-KG vector and purified as GST fusion proteins (Xiao et al., 1996): nucleotides 79–1557 (EGF repeats 1–13), nucleotides 1324–2808 (EGF repeats 11–24), nucleotides 2575–4008 (EGF repeats 22–34), and nucleotides 3751–5247 (EGF repeats 32–36, LNR repeats). Protein concentrations were determined by BCA protein assay kit (BioRad).

Coimmunoprecipitation and GST Pulldown Assays

Rat brain membrane samples were prepared as described (Xiao et al., 1996) and incubated overnight at 4°C with antibody-coupled Protein A agarose beads (Roche) or glutathione-agarose beads (Sigma) bound to GST-N1.1, N1.2, N1.3, or N1.4. Captured proteins were eluted from beads with SDS-PAGE sample buffer and subjected to Western blot and detection using ECL reagent (Amersham).

Lipid Raft Assay

Lipid raft assay was performed as described (Krämer et al., 1999).

Transfection of Cells

Cells were transfected using Lipofectamine (Invitrogen) as instructed.

Immunocytochemistry

Cells were cultured on 13 mm coverslips (Nalge Nunc International). After various treatments, including γ-secretase inhibitor (Sigma), cells were fixed with 4% paraformaldehyde and blocked with 1% BSA. Cells were then incubated with primary antibodies in 0.2% BSA for 1 hr, followed by Cy3-labeled or Cy2-labeled secondary antibody (Sigma). After mounting in fluorescent mounting medium (DAKO), cells were visualized with a Leica DM RXA2 fluorescent microscope. The photos were taken using the same optical parameters to ensure the comparable luminosity. At least ten different viewing fields from three independent experiments were used to calculate the percentage of cells showing NICD translocation or differentiation. Two hundred cells from at least three independent experiments were quantified for fluorescence intensities by Adobe Photoshop (Jack et al., 2001) and measured for cytoplasmic area by Leica QFluoro software. The raw data were analyzed by Student's t test with $p < 0.05$ and $p < 0.01$ being considered a significant or highly significant difference, respectively.

Cell Coculture

Parental or transfected CHO cells were cultured with OLN in a 2:1 ratio for 2 days. To study OLN cell processes, cells were prestained with the PKH26 red fluorescent cell linker kit (Sigma). Then OLN and CHO cells were stained for c-*myc*. Over 100 OLN cells in three randomly selected areas from three independent experiments were counted and the raw data were analyzed by Newman-Keuls test with $p < 0.05$ and $p < 0.01$ being considered a significant or highly significant difference, respectively.

Culture of Primary OLs and OPCs

Primary OLs were isolated from P5-7 rat brain cerebrum (Colello and Sato-Bigbee, 1998), and OPCs from P5-7 rat optic nerve (Bögler, 1997).

Real-Time PCR Analysis

Total RNA from OLs or OLN cells was extracted using the QIAGEN RNeasy kit and treated with RNase-free DNaseI (Invitrogen). Samples were used for reverse transcription with random hexamer primers using SuperScript First-Strand Synthesis System (Invitrogen) (Notch homologs, *Hes1*) or TaqMan RT Kit (Applied Biosystems) (MAG). β-actin and GAPDH were used as internal controls. Real-time PCR was performed using the SYBR Green PCR Master Mix (Notch homologs, *Hes1*) or TaqMan system (MAG) on an ABI PRISM 7700 Sequence Detection System. The primers and TaqMan probes were designed using Primer Express Software (ABI), and sequences are available upon request. The raw data from at least four independent experiments were used to determine the relative expression levels of each transcript by employing the comparative C_T method (ABI user's manual).

Hes1 Luciferase Reporter Assay

OLN cells (1.5×10^5/well) in 12-well dishes were used for *Hes1* luciferase reporter assays. Cells were transiently transfected using Lipofectamine and Lipofectamine Plus reagents (Invitrogen). Each well received pGVB/*Hes1* luciferase reporter plasmid together with various expression plasmids. The β-galactosidase expression plasmid pCMV/β-Gal was included as internal control. Cells were lysed 24 hr posttransfection and assayed using the Steady-Glo Luciferase Assay Kit (Promega). The raw data from at least four independent experiments were used to determine the relative reporter activity.

Acknowledgments

We particularly thank Dr. Jeffrey Nye for providing mouse Notch1 cDNA, and Dr. Genevieve Rougon for the F3-transfected CHO cell line and F3 antibody, and for extensive discussion on the project and critical review of the manuscript. We also thank Dr. Domna Karagogeos for providing TAG-1- and TAX-transfected CHO cell lines, Dr. Melanie Richter for CHL1-Fc, Dr. Urban Lendahl for Notch1, and Notch3 antibodies, Dr. Tetsuo Sudo (Toray, Japan) for Hes1 polyclonal antibody, Dr. Ryoichiro Kageyama for pGVB/Hes1 luciferase reporter construct, and Dr. Craig Heilman for wild-type RBP-J construct. We are particularly indebted to Alain Israel for long-term support and critique on our work and providing murine Notch1-transfected HeLa cells and NICD antibody. We sincerely thank Dr. Malcolm Paterson for insightful comments and revision of the manuscript. We are grateful to Dr. Yun-Jin Jiang for his valuable suggestion. This work was supported by grants from: (1) the National Medical Research Council of Singapore, Singapore Health Services Pte Ltd., and Department of Clinical Research, Singapore General Hospital to Z.C. Xiao; (2) Canadian Institutes of Health Research to C.J. Pallen; (3) the Hertie Foundation and the European Community to M. Schachner; and (4) NIH grants HL 35627, HL 32348, and RR 15555 to T. Maciag.

Received: December 26, 2002
Revised: September 24, 2003
Accepted: September 25, 2003
Published: October 16, 2003

References

Berglund, E.O., Murai, K.K., Fredette, B., Sekerkova, G., Marturano, B., Weber, L., Mugnaini, E., and Ranscht, B. (1999). Ataxia and abnormal cerebellar microorganization in mice with ablated contactin gene expression. Neuron *24*, 739–750.

Bögler, O. (1997). Isolation and purification of primary oligodendrocyte precursors. In Current Protocols in Neuroscience, J.N. Crawley, C. Gerfen, R. McKay, M. Rogawski, D.R. Sibley, and P. Skolnick, eds. (New York: John Wiley and Sons, Inc.), 3.4.1–3.4.9.

Colello, R.J., and Sato-Bigbee, C. (1998). Purification of oligodendrocytes and their progenitors using immunomagnetic separation

and percoll gradient centrifugation. In Current Protocols in Neuroscience, J.N. Crawley, C. Gerfen, R. McKay, M. Rogawski, D.R. Sibley, and P. Skolnick, eds. (New York: John Wiley and Sons, Inc.), 3.12.7–3.12.10.

Dale, J.K., and Maroto, M. (2003). A HES1-based oscillator in cultured cells and its potential implications for the segmentation clock. Bioessays *25*, 200–203.

Dawson, M.R., Levine, J.M., and Reynolds, R. (2000). NG2-expressing cells in the central nervous system: are they oligodendroglial progenitors? J. Neurosci. Res. *61*, 471–479.

Ebinu, J.O., and Yankner, B.A. (2002). A RIP tide in neuronal signal transduction. Neuron *34*, 499–502.

Faivre-Sarrailh, C., Gauthier, F., Denisenko-Nehrbass, N., Le Bivic, A., Rougon, G., and Girault, J.A. (2000). The glycosylphosphatidyl inositol-anchored adhesion molecule F3/contactin is required for surface transport of paranodin/contactin-associated protein (caspr). J. Cell Biol. *149*, 491–502.

Gennarini, G., Durbec, P., Boned, A., Rougon, G., and Goridis, C. (1991). Transfected F3/F11 neuronal cell surface protein mediates intercellular adhesion and promotes neurite outgrowth. Neuron *6*, 595–606.

Genoud, S., Lappe-Siefke, C., Goebbels, S., Radtke, F., Aguet, M., Scherer, S.S., Suter, U., Nave, K.A., and Mantei, N. (2002). Notch1 control of oligodendrocyte differentiation in the spinal cord. J. Cell Biol. *158*, 709–718.

Girault, J.A., and Peles, E. (2002). Development of nodes of Ranvier. Curr. Opin. Neurobiol. *12*, 476–485.

Hemann, C., Gartner, E., Weidle, U.H., and Grummt, F. (1994). High-copy expression vector based on amplification-promoting sequences. DNA Cell Biol. *13*, 437–445.

Hirata, H., Yoshiura, S., Ohtsuka, T., Bessho, Y., Harada, T., Yoshikawa, K., and Kageyama, R. (2002). Oscillatory expression of the bHLH factor Hes1 regulated by a negative feedback loop. Science *298*, 840–843.

Holm, J., Hillenbrand, R., Steuber, V., Bartsch, U., Moos, M., Lubbert, H., Montag, D., and Schachner, M. (1996). Structural features of a close homologue of L1 (CHL1) in the mouse: a new member of the L1 family of neural recognition molecules. Eur. J. Neurosci. *8*, 1613–1629.

Huppert, S.S., Le, A., Schroeter, E.H., Mumm, J.S., Saxena, M.T., Milner, L.A., and Kopan, R. (2000). Embryonic lethality in mice homozygous for a processing-deficient allele of Notch1. Nature *405*, 966–970.

Izon, D.J., Aster, J.C., He, Y., Weng, A., Karnell, F.G., Patriub, V., Xu, L., Bakkour, S., Rodriguez, C., Allman, D., and Pear, W.S. (2002). Deltex1 redirects lymphoid progenitors to the B cell lineage by antagonizing Notch1. Immunity *16*, 231–243.

Jack, C., Berezovska, O., Wolfe, M.S., and Hyman, B.T. (2001). Effect of PS1 deficiency and an APP gamma-secretase inhibitor on Notch1 signaling in primary mammalian neurons. Brain Res. Mol. Brain Res. *87*, 166–174.

John, G.R., Shankar, S.L., Shafit-Zagardo, B., Massimi, A., Lee, S.C., Raine, C.S., and Brosnan, C.F. (2002). Multiple sclerosis: Re-expression of a developmental pathway that restricts oligodendrocyte maturation. Nat. Med. *8*, 1115–1121.

Kabos, P., Kabosova, A., and Neuman, T. (2002). Blocking HES1 expression initiates GABAergic differentiation and induces the expression of p21 (CIP1/WAF1) in human neural stem cells. J. Biol. Chem. *277*, 8763–8766.

Kaneta, M., Osawa, M., Sudo, K., Nakauchi, H., Farr, A.G., and Takahama, Y. (2000). A role for pref-1 and HES-1 in thymocyte development. J. Immunol. *164*, 256–264.

Kato, H., Taniguchi, Y., Kurooka, H., Minoguchi, S., Sakai, T., Nomura-Okazaki, S., Tamura, K., and Honjo, T. (1997). Involvement of RBP-J in biological functions of mouse Notch1 and its derivatives. Development *124*, 4133–4141.

Kazarinova-Noyes, K., Malhotra, J.D., McEwen, D.P., Mattei, L.N., Berglund, E.O., Ranscht, B., Levinson, S.R., Schachner, M., Shrager, P., Isom, L.L., and Xiao, Z.C. (2001). Contactin associates with Na^+ channels and increase their functional expression. J. Neurosci. *21*, 7517–7525.

Kishi, N., Tang, Z., Maeda, Y., Hirai, A., Mo, R., Ito, M., Suzuki, S., Nakao, K., Kinoshita, T., Kadesch, T., et al. (2001). Murine homologs of deltex define a novel gene family involved in vertebrate Notch signaling and neurogenesis. Int. J. Dev. Neurosci. *19*, 21–35.

Klein, C., Kramer, E.M., Cardine, A.M., Schraven, B., Brandt, R., and Trotter, J. (2002). Process outgrowth of oligodendrocytes is promoted by interaction of fyn kinase with the cytoskeletal protein tau. J. Neurosci. *22*, 698–707.

Koch, T., Brugger, T., Bach, A., Gennarini, G., and Trotter, J. (1997). Expression of the immunoglobulin superfamily cell adhesion molecule F3 by oligodendrocyte-lineage cells. Glia *19*, 199–212.

Krämer, E.M., Klein, C., Koch, T., Boytinck, M., and Trotter, J. (1999). Compartmentation of Fyn kinase with glycosylphosphatidylinositol-anchored molecules in oligodendrocytes facilitates kinase activation during myelination. J. Biol. Chem. *274*, 29042–29049.

Lardelli, M., Dahlstrand, J., and Lendahl, U. (1994). The novel Notch homologue mouse Notch3 lacks specific epidermal growth factor-repeats and is expressed in proliferating neuroepithelium. Mech. Dev. *46*, 123–136.

Logeat, F., Bessia, C., Brou, C., LeBail, O., Jarriault, S., Seidah, N.G., and Israel, A. (1998). The Notch1 receptor is cleaved constitutively by a furin-like convertase. Proc. Natl. Acad. Sci. USA *95*, 8108–8112.

Martinez Arias, A., Zecchini, V., and Brennan, K. (2002). CSL-independent Notch signaling: a checkpoint in cell fate decisions during development? Curr. Opin. Genet. Dev. *12*, 524–533.

Matsuno, K., Ito, M., Hori, K., Miyashita, F., Suzuki, S., Kishi, N., Artavanis-Tsakonas, S., and Okano, H. (2002). Involvement of a proline-rich motif and RING-H2 finger of Deltex in the regulation of Notch signaling. Development *129*, 1049–1059.

Rand, M.D., Grimm, L.M., Artavanis-Tsakonas, S., Patriub, V., Blacklow, S.C., Sklar, J., and Aster, J.C. (2000). Calcium depletion dissociates and activates heterodimeric Notch receptors. Mol. Cell. Biol. *20*, 1825–1835.

Rebay, I., Fleming, R.J., Fehon, R.G., Cherbas, L., Cherbas, P., and Artavanis-Tsakonas, S. (1991). Specific EGF repeats of Notch mediate interactions with Delta and Serrate: implications for Notch as a multifunctional receptor. Cell *67*, 687–699.

Revest, J.M., Faivre-Sarrailh, C., Schachner, M., and Rougon, G. (1999). Bidirectional signaling between neurons and glial cells via the F3 neuronal adhesion molecule. Adv. Exp. Med. Biol. *468*, 309–318.

Richter-Landsberg, C., and Heinrich, M. (1996). OLN-93: a new permanent oligodendroglia cell line derived from primary rat brain glial cultures. J. Neurosci. Res. *45*, 161–173.

Sakurai, T., Lustig, M., Nativ, M., Hemperly, J.J., Schlessinger, J., Peles, E., and Grumet, M. (1997). Induction of neurite outgrowth through contactin and Nr-CAM by extracellular regions of glial receptor tyrosine phosphatase beta. J. Cell Biol. *136*, 907–918.

Schroeter, E.H., Kisslinger, J.A., and Kopan, R. (1998). Notch-1 signaling requires ligand-induced proteolytic release of intracellular domain. Nature *393*, 382–386.

Shimazaki, K., Hosoya, H., Takeda, Y., Kobayashi, S., and Watanabe, K. (1998). Age-related decline of F3/contactin in rat hippocampus. Neurosci. Lett. *245*, 117–120.

Shimizu, K., Chiba, S., Kumano, K., Hosoya, N., Takahashi, T., Kanda, Y., Hamada, Y., Yazaki, Y., and Hirai, H. (1999). Mouse jagged1 physically interacts with notch2 and other notch receptors. Assessment by quantitative methods. J. Biol. Chem. *274*, 32961–32969.

Small, D., Kovalenko, D., Kacer, D., Liaw, L., Landriscina, M., Di Serio, C., Prudovsky, I., and Maciag, T. (2001). Soluble Jagged 1 represses the function of its transmembrane form to induce the formation of the Src-dependent chord-like phenotype. J. Biol. Chem. *276*, 32022–32030.

Tsiotra, P.C., Karagogeos, D., Theodorakis, K., Michaelidis, T.M., Modi, W.S., Furley, A.J., Jessell, T.M., and Papamatheakis, J. (1993). Isolation of the cDNA and chromosomal localization of the gene

(TAX1) encoding the human axonal glycoprotein TAG-1. Genomics *18*, 562–567.

Umemori, H., Sato, S., Yagi, T., Aizawa, S., and Yamamoto, T. (1994). Initial events of myelination involve Fyn tyrosine kinase signaling. Nature *367*, 572–576.

Wang, S., Sdrulla, A.D., diSibio, G., Bush, G., Nofziger, D., Hicks, C., Weinmaster, G., and Barres, B.A. (1998). Notch receptor activation inhibits oligodendrocyte differentiation. Neuron *21*, 63–75.

Xiao, Z.C., Taylor, J., Montag, D., Rougon, G., and Schachner, M. (1996). Distinct effects of recombinant tenascin-R domains in neuronal cell functions and identification of the domain interacting with the neuronal recognition molecule F3/11. Eur. J. Neurosci. *8*, 766–782.

Yamamoto, N., Yamamoto, S., Inagaki, F., Kawaichi, M., Fukamizu, A., Kishi, N., Matsuno, K., Nakamura, K., Weinmaster, G., Okano, H., and Nakafuku, M. (2001). Role of Deltex-1 as a transcriptional regulator downstream of the Notch receptor. J. Biol. Chem. *276*, 45031–45040.

Zeng, L., D'Alessandri, L., Kalousek, M.B., Vaughan, L., and Pallen, C.J. (1999). Protein tyrosine phosphatase alpha (PTPalpha) and contactin form a novel neuronal receptor complex linked to the intracellular tyrosine kinase fyn. J. Cell Biol. *147*, 707–714.

Immunity, Vol. 20, 87–93, January, 2004, Copyright ©2004 by Cell Press

Unexpectedly Efficient Homing Capacity of Purified Murine Hematopoietic Stem Cells

Yumi Matsuzaki,[1,2,3,*] Kentaro Kinjo,[1,4] Richard C. Mulligan,[2] and Hideyuki Okano[1,3,*]
[1]Department of Physiology
Keio University School of Medicine
35 Shinanomachi, Shinjuku-ku
Tokyo 160-8582
Japan
[2]Department of Molecular Medicine
Children's Hospital and Department of Genetics
Harvard Medical School
Boston, Massachusetts 02115
[3]Core Research for Evolutional Science and Technology (CREST)
Japan Science and Technology Corporation (JST)
4-1-8, Honcho, Kawaguchi
Saitama 332-0012
Japan
[4]Division of Hematology
Department of Internal Medicine
Keio University School of Medicine
35 Shinanomachi, Shinjuku-ku
Tokyo 160-8582
Japan

Summary

Single-cell transplantation analysis revealed that the cells that had the strongest dye efflux activity ("Tip"-SP cells) and had the phenotype CD34− c-Kit+ Sca-1+ Lin− (CD34− KSL cells) exhibited very strong proliferation and multilineage differentiation capacity. Ninety-six percent of the lethally irradiated mice that received a single "Tip"-SP CD34− KSL cell showed significant donor cell engraftment for long term. These findings support the hypothesis that "Tip"-SP CD34− KSL cells represent the most primitive hematopoietic stem cells that are capable of migrating into the primary site and surviving and/or proliferating with nearly absolute efficiency. This led us to propose high marrow-seeding efficiency as a specific characteristic of primitive HSCs, in addition to their self-renewal and multipotent capacity.

Introduction

Hematopoietic stem cells (HSCs) are defined as having both the capacity for self renewal and the ability to differentiate into all mature hematopoietic lineages. The most compelling experimental evidence for the existence of such cells is the ability of bone marrow-derived cells to reconstitute the hematopoietic system of lethally irradiated recipients long term (Jones et al., 1990; Metcalf, 1971; Till and McCulloch, 1961).

The identification of molecular markers that characterize transplantable cells with stem cell potential and allow their selective purification is an achievement that has been important to progress in many applied and basic studies (Goodell et al., 1996; Osawa et al., 1996a; Spangrude et al., 1988). As a result of a series of studies by different investigators, the most primitive HSCs have been identified as being CD34−, c-Kit+, Sca-1+, and Lin− (Osawa et al., 1996a; Smith et al., 1991; Spangrude et al., 1995; Uchida et al., 1996), and these cells eventually give rise to a significant number of donor-derived myelo-lymphoid cells. However, even in the best case series reported, only one in five recipients showed successful engraftment after single-cell transplantation (Osawa et al., 1996a). The results in that series suggest either that the other four cells were not HSCs or that the fraction was pure, but only a portion of the cells injected reached a site in vivo where their regenerative potential could be activated. Since values of approximately 10% to 20% have been obtained for the marrow-seeding efficiency of related populations based on measurements of the 24 hr bone marrow seeding or spleen colony-forming units (Hendrikx et al., 1996; Lanzkron et al., 1999; Oostendorp et al., 2000; van der Loo and Ploemacher, 1995; von Melchner and Metcalf, 1980), likely in vivo bone marrow transplantation assays are underestimateing the number of cells with HSC potential.

We previously described a method of isolating murine HSCs by dual-wavelength flow cytometric analysis with the fluorescent DNA binding dye Hoechst 33342 (Goodell et al., 1996, 1997). This method relies on the differential ability of stem cells to efflux the Hoechst dye, which, like the activity of P-glycoprotein (Scharenberg et al., 2002; Zhou et al., 2001), defines a small subset of side population (SP) cells. The isolated murine bone marrow SP cell population was shown to be in cells with lymphoid and myeloid hematopoietic reconstituting activity in vivo (Goodell et al., 1996, 1997).

In this report, we describe a method of further purifying HSCs by combining staining with fluorochrome-conjugated antibodies to cell surface antigens with Hoechst dye efflux analysis. After single-cell transplantation of the cells isolated, donor-derived cells were detected in almost all of the recipient animals and multilineage reconstitution was observed. Thus, we obtained direct evidence that the fraction isolated possesses the phenotype of the most primitive HSCs and that a single HSC is capable of repopulating bone marrow with nearly absolute efficiency. Our results also showed that HSCs have an unexpectedly high ability to home to the appropriate site for their survival and/or proliferation, which may be another important characteristic of stem cells.

Results

The Cells with the Strongest Dye Efflux Ability Showed the Highest Marrow Repopulating Potency

As stated above, the side population (SP) is a rare population of cells in murine bone marrow (Goodell et al., 1996) and is characterized by low blue and low red fluorescence intensity when examined by dual wave-

*Correspondence: penguin@sc.itc.keio.ac.jp (Y.M.), hidokano@sc.itc.keio.ac.jp (H.O.)

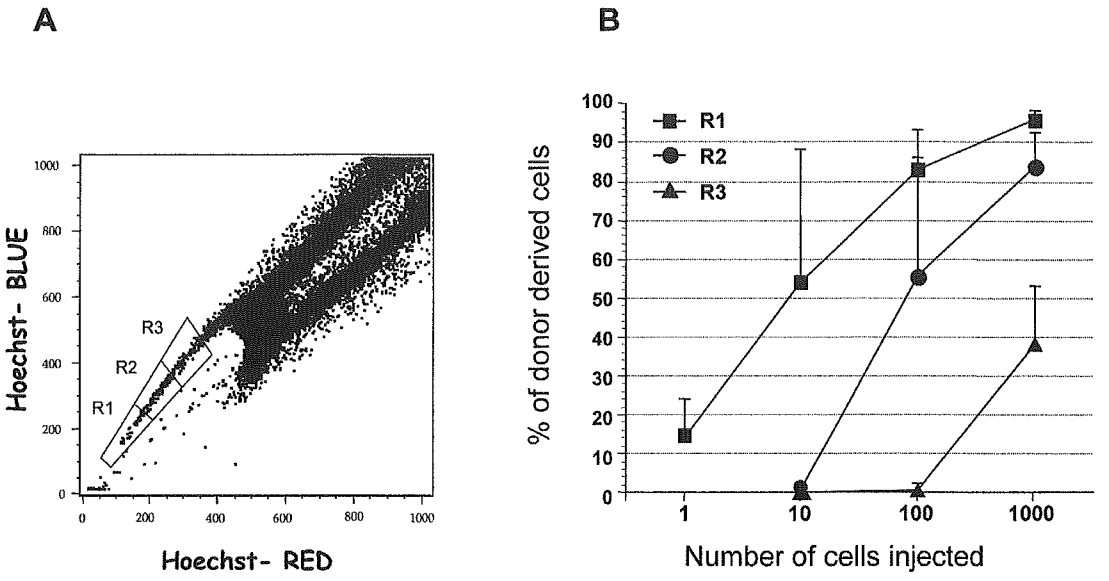

Figure 1. Hoechst Dye Efflux from Mouse Bone Marrow Cells

A representative flow cytometric profile of unfractionated bone marrow mononuclear cells stained with Hoechst 33342.

(A) The region indicated defines the SP cells. Subfractions of SP cells (R1–R3) are also indicated. R1 represents 0.02%–0.07% of the cell population, R2 about 0.1%, and R3 about 0.3%.

(B) Engraftment activity of the SP subfractions. Competitive repopulation with serially diluted subfractions of the SP cells was attempted. The percentages of GFP+ donor-derived cells detected in the peripheral blood of recipient mice 12 weeks after transplantation with R1, R2, or R3 cells are shown. The values shown are the means ± SD of three independent experiments on 10–20 animals per trial. The percentages of donor cells in animals that were injected with a single R1 cell were calculated for the animals that showed >1% chimerism.

length fluorescence of blue versus red detected at 405 and 585 nm, respectively. This population generally represents 0.5% of ficoll-isolated mononuclear bone marrow cells (range 0.2%–0.8%, n > 30) (Figure 1A). The regions indicated (R1–R3) were defined based on a dye efflux gradient, in which R1 cells had the highest dye efflux and R3 the lowest. We previously reported observing that cells with the highest dye efflux (or lowest staining) had the greatest long-term repopulating ability (Goodell et al., 1997). As a first step in extending those previous findings, we attempted to confirm the relative potency of the different subfractions of the SP population and further quantitate the efficiency of reconstitution of those fractions by transplantation of different numbers of cells (including single cells) in the presence of unfractionated competitor bone marrow cells. The purified SP cells used for these studies were derived from the CAG-EGFP transgenic mice (see Experimental Procedures). Twelve weeks after transplantation, peripheral blood cells were collected from individual recipients and analyzed for EGFP expression as a marker for the donor-derived cells. The results are shown in Figure 1B, and the data clearly reveal that the R1 fraction had stronger marrow repopulating activity than the R2 or R3 fraction. We refer to the R1 fraction as "Tip"-SP cells. When lethally irradiated mice were injected with a single R1 cell, one out of five recipients was positive for a significant number of donor-derived cells (n = 21) and had occurred engraftment in all mice that received 10 or more cells per injection, whereas 1000 cells were required for repopulation by the R3 fraction.

The data clearly support our earlier finding that the fraction of cells with the strongest dye efflux activity has the highest marrow-repopulating activity, and the engraftment efficiency (1/5) in the present study was as high as that reported for CD34− KSL cells (Osawa et al., 1996a). However, because the engraftment efficiency was still not absolute, we performed a detailed phenotype analysis of the "Tip"-SP cells.

SP Cells in Murine Bone Marrow Are Phenotypically Heterogeneous

The surface phenotype analysis showed that the "Tip"-SP cells (Figure 2A, left) were positive for c-Kit (>98%, n > 30) and mostly negative for lineage markers (<2%, n > 30) (Figure 2B, left), suggesting that SP cells are homogeneous with respect to c-Kit and Lin expression. However, a representative two-dimensional profile of Sca-1/CD34 showed that the "Tip"-SP cells were a mixed population (Figure 2B, right). Interestingly, the proportion of CD34− Sca-1+ within the "Tip"-SP cell population was about 20% (range 8%–25%, n > 30). The frequency of "Tip"-SP cells within the CD34− KSL cells population is also about 20% (range 10%–30%, n > 30) (Figure 2A, right). Although the marrow-repopulating efficiency of these two sets of cells is almost equal, the "Tip"-SP fraction overlaps only 20% of the CD34− KSL population. As a result, these populations are not equivalent.

We then performed a competitive marrow-repopulation assay to assess the characteristics of each SP subset. One hundred cells of unfractionated SP cells or SP

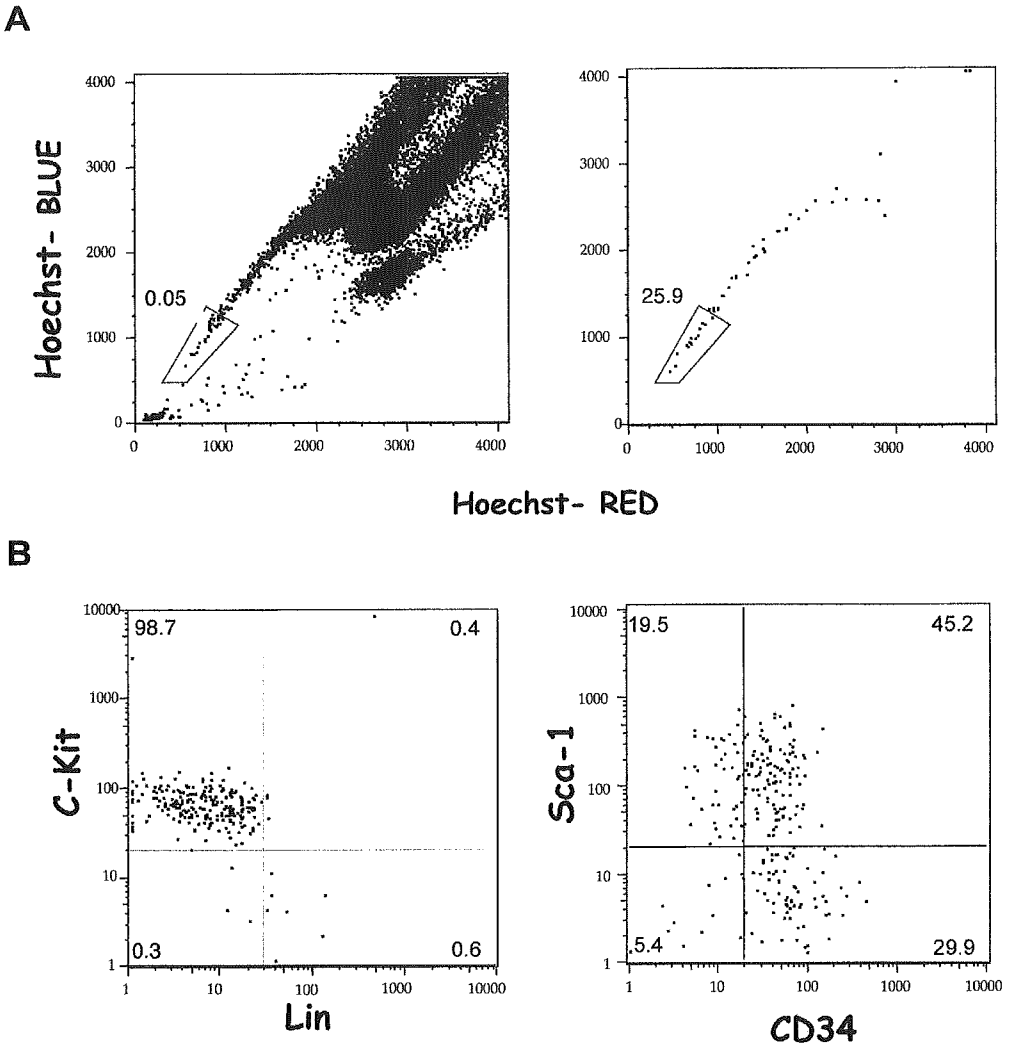

Figure 2. Characterization of Mouse Bone Marrow SP Cells

Representative flow cytometric profile of Hoechst 33342- and antibody-stained cells.

(A) Hoechst fluorescence of mouse bone marrow mononuclear cells. The "Tip"-SP cells were gated with a blue polygon. The value shown is the percentage of the cells in each region (left). Hoechst fluorescence of CD34− Sca-1+ c-Kit+ Lin− cells. The "Tip"-SP region drawn is identical to that in the left panel (right).

(B) c-Kit and lineage marker profile of the "Tip"-SP cells (the region indicated in [A]) (left). Sca-1 and CD34 profile of the "Tip"-SP cells (right).

subset cells from C57 BL/6-Ly5.1 donor animals together with 1×10^6 of unfractionated bone marrow cells from wild-type C57BL/6-Ly5.2 animals were injected into lethally irradiated C57BL/6-Ly5.2 recipients. Two, four, and eight weeks after the injection, peripheral blood was retroorbitally collected from the recipients, and the mononuclear cells were analyzed for the presence of donor-derived (Ly5.1 positive) cells by flow cytometry. The data from a representative experiment are shown in Table 1.

The recipients that were injected with the unfractionated SP cells contained a certain number of donor-derived (Ly5.1 positive) cells every time specimens were collected. Repopulation by CD34+ Sca-1+ SP cells was only short term, with the donor cells only being detected at 2–4 weeks after transplantation and disappearing by 8 weeks. No cells derived from the CD34− Sca-1+ SP cells were detected at 2 weeks, but some were detected after 4 weeks, and their frequency increased over time. By contrast, the repopulation by CD34− Sca-1+ non-SP cells was only short term (data not shown). The population of Sca-1 negative cells did not exhibit any marrow-repopulating activity.

The data strongly suggested that CD34− KSL SP cells represent long-term marrow-repopulating activity and that CD34+ KSL SP cells represent short-term engraftment. A cobblestone area-forming assay in a recent study by another group also revealed that SP cells are

Table 1. Percentage of Donor-Derived GFP-Positive Cells after Transplantation of SP Cell Subsets

Phenotype[b]	Cells Per Mouse[c]	% Donor-Derived Ly5.1+ Cells[a]		
		2 Weeks[d]	4 Weeks	8 Weeks
Total SP	100	39.2 ± 5.9	14.7 ± 2.7	23.2 ± 5.5
CD34(+) Sca-1(+) SP	100	22.4 ± 5.7	4.5 ± 0.8	0.5 ± 0.8
CD34(−) Sca-1(+) SP	100	2.1 ± 0.9	17.3 ± 8.0	34.7 ± 18.5
Sca-1(−) SP	1000	0 ± 0	0 ± 0	0 ± 0

Values shown are mean ± SD.
[a]Donor-derived cells in the peripheral blood of recipient mice were detected by flow cytometric analysis, and the percentage of Ly5.1-positive donor-derived cells was measured. The results are shown as the mean ± SD.
[b]All subfractions were isolated by flow cytometric analysis and sorted as described in the Experimental Procedures.
[c]The number of cells indicated was injected with 2×10^5 of unfractionated wild-type bone marrow cells.
[d]Peripheral blood specimens were collected from the recipient mice at the times indicated.

a mixed population and that CD34− Sca-1+ SP cells have long-term repopulating ability (Parmar et al., 2003). Taking all of the above into consideration, we concluded that the fraction of cells exhibiting the "Tip"-SP and CD34− KSL are the most primitive HSCs.

"Tip"-SP CD34− KSL Cells Exhibited a Capacity for Multilineage, Long-Term Repopulation and Possessed High Marrow-Seeding Efficiency

To test their long-term and multilineage reconstitution potency, we performed a competitive repopulation assay of single "Tip"-SP CD34− KSL cells, which are extremely rare, representing only 0.001%–0.01% of ficoll-isolated bone marrow mononuclear cells. "Tip"-SP CD34− KSL cells from CAG-EGFP transgenic mice were transplanted into lethally irradiated wild-type C57BL/6 mice, as one cell per recipient, together with 1×10^5 unfractionated bone marrow cells derived from C57BL/6 mice (see Experimental Procedures). The results of three independent experiments are shown in Figure 3. Donor-derived GFP-positive cells were detectable (>1%) in 70 of 73 recipients (95.9%), and 68 of 73 (93%) of the host animals exhibited >10% chimerism at 12 weeks after transplantation. Surprisingly, EGFP-positive cells of donor origin accounted for >1% of the peripheral blood cells of all recipients in Experiment 3. The mean percentage of EGFP-positive donor cells was 44.7 ± 24.7% (n = 73), indicating that the chimerisms were significantly diverse (range 0.5%–82%).

A lineage analysis of peripheral blood cells from recipient animals was also performed, and the representative data from Experiment 3 are shown in Table 2. Both myelo/monocytes and T/B lymphocytes derived from a single "Tip"-SP cell were detected in each recipient at 3, 6, and 12 months after transplantation.

We therefore concluded that, based on the definition of long-term marrow repopulating potency and multilineage differentiation, over 90% of the "Tip"-SP CD34− KSL cells should be the most primitive hematopoietic stem cells.

Discussion

The definition of pluripotential hematopoietic stem cells has two parts: each stem cell must be capable of giving rise to progeny in all defined myelo/lymphoid lineages and limiting numbers of stem cells must be capable of fully reconstituting lethally irradiated mice, leading to the establishment of long-term hematopoietic repopulation. The results of the present study clearly demonstrated that a single "Tip"-SP CD34− KSL cell gave rise to all defined lineages and that a single cell was sufficient to restore long-term hematopoiesis in lethally irradiated mice.

Several groups have reported that the spleen is the primary site of stem cell expansion after transplantation (Osawa et al., 1996b) and estimated that the spleen seeding factor (*f*) is 0.1 to 0.2 (Spangrude et al., 1995; van der Loo and Ploemacher, 1995). On the other hand, it has recently been reported that an stem cell fraction isolated from mouse and human HSCs possesses high marrow-seeding efficiency (Benveniste et al., 2003; Cashman and Eaves, 2000). Our findings in this study directly support the findings in these recent reports,

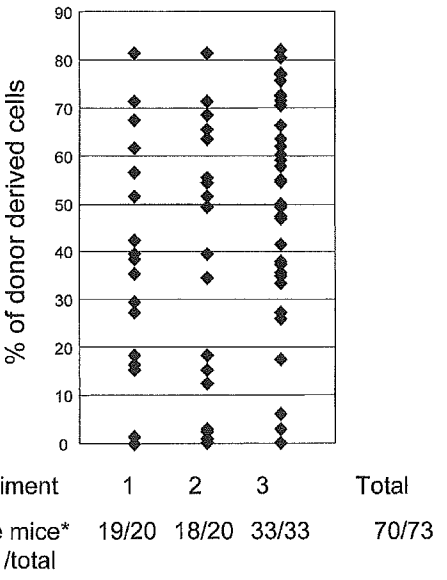

Figure 3. Results of Bone Marrow Reconstitution by Single "Tip"-SP CD34− KSL Cells

The peripheral blood cells of recipient mice were analyzed 12 weeks after transplantation. The chimerism of donor-derived cells was calculated as the % of GFP+/% of all live cells. Each dot (◆) represents the percentage of donor-derived cells in each recipient.

Table 2. Lineage Analysis for Single "Tip"-SP CD34− KSL-Derived Cells from the Peripheral Blood Cells of Recipient Animals

Months[a]	N[b]	Total[c]	Myeloid[d]	Lymphoid[e]
3	33	53.3 ± 23.1	15.0 ± 8.5	83.6 ± 10.8
6	18	49.1 ± 32.8	21.5 ± 17.2	75.9 ± 19.1
12	18	47.6 ± 31.3	24.9 ± 17.5	74.7 ± 18.5

Donor-derived cells in the peripheral blood of recipient mice were detected by flow cytometric analysis, and the percentage of EGFP-positive donor-derived cells was measured. Values shown are mean ± SD.

[a] Months after transplantation.

[b] Number of recipients. The numbers of mice were lower at 6 months because some animals were sacrificed to determine the distribution of EGFP-positive donor cells in nonhematopoietic organs (our unpublished data).

[c] Mean percentage of total EGFP-positive donor-derived cells.

[d] Mean percentage of EGFP-positive donor-derived cells that were myeloid (Gr-1/Mac-1 positive) cells.

[e] The mean percentage of EGFP-positive donor-derived cells that were T or B (CD3/B220-positive) cells.

since a single "Tip"-SP CD34− KSL cell was seeded in almost every animal, suggesting that the most primitive HSCs have an extremely high capacity home to the site that supports their survival and expansion.

If cells capable of long-term multilineage repopulation but without any homing capacity existed, they would not exhibit strong engraftment in any ordinary intravenous transplantation assay; however, they might be capable of long-term and multilineage reconstitution if injected directly into the bone marrow. Future studies should be designed to identify the molecules and mechanisms required for homing of hematopoietic stem cells in vivo. In view of the above, we propose that the definition of HSCs should include homing capacity as well as multilineage differentiation and self-renewal capacity. The primary lodging site of pure HSCs and their homing capacity should be determined after transplantation by means of in vivo imaging and a luciferase reporter signal (Collaco and Geusz, 2003).

Although the engraftment efficiency of the "Tip"-SP CD34− KSL cells was extremely high, the percentage of donor cells varied significantly between individual recipients. This raises two possibilities: that the HSC populations used in this study may have had equally efficient homing capacity but had heterogeneous proliferation potency and, second, that the cells were homogenous in regard to both homing and proliferation capacity, but their regenerative potential may depend on the microenvironment in which the individual transplanted cells settled.

Our results may introduce additional interesting nature of HSCs in regard to the fate determination of HSCs. If the lineage commitment is determined by a stochastic mechanism, whatever the self renew to commitment ratio, the probability of engraftment would never reach 100%. Our data indicated that a single transplanted "Tip"-SP CD34− KSL cell repopulated each recipient long term with absolute engraftment efficiency, and thus, all of the cells must have self renewed during the first cell division. As described previously, the lineage commitment of HSCs has been regarded as a stochastic process, but it may be modified by extrinsic signals from the microenvironment (Metcalf, 1999).

In our previous studies, a majority of cells within the SP cell population were negative/low for CD34 but positive for Sca-1. The results of the current study, however, suggest that optimal antibody staining conditions can be used to resolve several rare subpopulations of SP cells on the basis of expression of CD34 and Sca-1. We had tested various staining conditions for the antibodies used in the present experiment and had found that the saturation point of the anti-CD34 antibody was 5 μg/ml, five times higher than that of the others, and that the same concentration of isotype control antibody did not affect the background staining level (Y.M. and R.C.M., unpublished data). On the basis of those studies, we conclude that the CD34 expression detected under the condition used in the present study was due to specific binding of the CD34 cell surface antigen. "Tip"-SP cells purified under these optimal conditions can be distinguished from other SP cells on the basis of their extraordinarily high specific reconstitution activity and thus they must possess a strong ability to home to sites in vivo compatible within sustained hematopoiesis.

Experimental Procedures

Mice

C57BL/6 mice 8–10 weeks of age were purchased at from CLEA Japan, Inc. (Tokyo, Japan). C57BL/6 transgenic mice that ubiquitously express enhanced green fluorescent protein (EGFP) under the control of the CAG promoter (Kawamoto et al., 2000) were kindly provided from Dr. Jun-ichi Miyazaki (Osaka University, Osaka Japan) and were bred in our animal facility. The mice were kept under specific pathogen-free conditions in our animal facility at Keio University School of Medicine. All transgenic mice used in this study were heterozygous for the transgene.

Some C57BL/6 mice and all of the B6.SJL-Ptprca Pep3b/BoyJ (C57BL/6-Ly5.1) were purchased at 8–10 weeks of age from Jackson laboratory (Bar Harbor, Maine). These mice were kept under specific pathogen-free conditions in the animal facility at Harvard University Medical School.

Preparation of Bone Marrow Cells and Hoechst 33342 Staining

Donor mice were sacrificed by cervical dislocation, the femurs and tibias were dissected out, and single-cell suspension was prepared as follows. The bones were crushed with a pestle, and the marrow cells were suspended in HBSS+ (calcium- and magnesium-free Hanks-balanced salt solution supplemented with 2% FCS, 10 mM HEPES, and 1% penicillin/streptomycin), and the cell suspensions were filtered through a cell strainer (Falcon 2350) to remove debris. The filtrate was suspended in 50 ml of ice-cold HBSS+ and then pelleted by centrifugation at 280 *g* for 6 min at 4°C. The bone marrow cells were resuspended at 1×10^6 cells/ml in HBSS+ and then incubated with 5 μg/ml Hoechst 33342 (Sigma Chemical Co., St. Louis, MO) for 60 min at 37°C. A parallel aliquot was stained with the Hoechst dye in the presence of 50 μM reserpine (Sigma Chemical Co.). We noticed that Hoechst 33342 staining is not always reproducible, and since the staining profiles of different batches of the dye varied considerably, we screened several Hoechst 33342 dyes to select a suitable batch, and ultimately chose lot number 31K4028 for use in the experiments.

After Hoechst staining, the cells were spun again, resuspended in 5 ml of ice-cold HBSS+, and layered on top of 5 ml of Ficoll-Paque™ Plus (Amersham Pharmacia Biotech AB, Uppsala, Sweden). After a centrifugation at 630 *g* at 4°C for 20 min, the mononuclear cells were recovered from the intermediate layer and immediately washed with 10 ml of ice-cold HBSS+.

Antibody Staining

The Hoechst-stained cells were resuspended in ice-cold HBSS+ at $1–5 \times 10^7$ cells/ml, then stained for 30 min on ice with the following mAbs: biotinylated CD34 (RAM34), PE-conjugated Sca-1 (Ly6A/E),

APC-conjugated c-Kit (ACK2), and PE-Cy5-conjugated lineage markers (Gr-1: RB6-8C5, Mac-1: M1-70, B220: RA3-6B2, CD3: 145-2C11, TER119). Biotinylated antibodies were visualized with Cy7-APC-conjugated streptavidin. All of these reagents were purchased from PharMingen (San Diego, CA) or e-Bioscience (San Diego, CA). An aliquot of cells was also stained with a mouse isotype control conjugated with FITC, PE, or APC. After antibody staining, the cells were washed with an excess amount of HBSS+ and resuspended at 1×10^7 cells/ml in HBSS+ containing 2 μg/ml propidium iodide (PI; Sigma Chemical Co.).

Flow Cytometry

Cell analysis and sorting were performed on a triple laser MoFlo (Cytomation, CO) with Summit software. Hoechst 33342 was excited at 350 nm, and fluorescence emission was detected by using a 405/BP30 and 570/BP20 optical filter for Hoechst blue and Hoechst red, respectively, and a 550 nm long-pass dichroic mirror (all Omega Optical Inc.) to separate the emission wavelengths. Both Hoechst blue and red fluorescence are shown on a linear scale. PI fluorescence was measured through 630BP30 after excitation at 488 nm with an argon laser, and a live cell gate was defined that excluded the cells positive for PI. After collecting 1×10^5 events, the SP population was defined as shown in a previous report (Goodell et al., 1996). Additional gates were defined as positive for Sca-1 and c-Kit and negative for CD34 and Lin, according to the negative control fluorescence intensity. Populations of CD34− Sca-1+ c-Kit+ Lin− SP bone marrow cells that are 99% pure are routinely prepared by this method.

Single Hematopoietic Stem Cell Transplantation

CD34− Sca-1+ c-Kit+ Lin− "Tip"-SP cells derived from donor CAG-GFP transgenic animals were sorted directly into separate wells of a 96 well plate containing 100 μl of HBSS+ by a CyClone automated cell deposition unit. Calibration of the clone sorting with fluorescent beads has shown that <1% of the wells received more or less than one bead. A 100 μl of unfractionated marrow cell suspension (2×10^5 cells) from donors not carrying the CAG-GFP transgene was added to each well to serve as competitor cells. The contents of each well were then intravenously injected into the retroorbital plexus of etherized recipient mice that had been lethally irradiated with a dose of 10.5 Gy (200 μl per mouse). A different syringe was used for each well to prevent crosscontamination between wells.

Analysis for Donor Cell Repopulation

Peripheral blood samples were collected, and most of the erythrocytes were removed with Ficoll-Paque. The remaining cells were stained with the following reagents: PE-anti-Mac-1 plus PE-anti-Gr-1, and APC-anti-CD3 plus APC-anti-B220, or APC-anti-CD45. When the B6-Ly5.1 animals were used as a donor, the peripheral blood cells were also stained with FITC-conjugated anti-CD45.1 (Ly5.1) monoclonal antibody (clone A20, Pharmingen). Dual-laser FACS analysis was performed with a FACS Calibur (Becton and Dickinson, CA). Single HSC-derived cells were identified by the fluorescence intensity of either EGFP or Ly5.1-FITC. A mouse was considered positive for single HSC engraftment if it was positive for both donor-derived lymphoid and myeloid cells with >1% percentage. The frequencies of each fraction were calculated with FlowJo software (www.treestar.com).

Acknowledgments

We thank Drs. Toshio Suda and Seiji Okada for useful comments and discussions. We also thank Hiroko Kohike for technical assistance; and Kumiko Inoue and Akiyo Hirayama for excellent secretarial assistance. This work was supported in part by grants from Core Research for Evolutional Science and Technology (CREST) of the Japan Science and Technology Corporation; from the Ministry of Education, Science, and Culture of Japan to H.O. and Y.M.; and a grant-in-aid from the 21st Century COE program of the Ministry of Education, Science, and Culture of Japan to Keio University.

Received: August 18, 2003
Revised: December 3, 2003
Accepted: December 10, 2003
Published: January 20, 2004

References

Benveniste, P., Cantin, C., Hyam, D., and Iscove, N.N. (2003). Hematopoietic stem cells engraft in mice with absolute efficiency. Nat. Immunol. *4*, 708–713.

Cashman, J.D., and Eaves, C.J. (2000). High marrow seeding efficiency of human lymphomyeloid repopulating cells in irradiated NOD/SCID mice. Blood *96*, 3979–3981.

Collaco, A., and Geusz, M. (2003). Monitoring immediate-early gene expression through firefly luciferase imaging of HRS/J hairless mice. BMC Physiol. *3*, 8–18.

Goodell, M.A., Brose, K., Paradis, G., Conner, A.S., and Mulligan, R.C. (1996). Isolation and functional properties of murine hematopoietic stem cells that are replicating in vivo. J. Exp. Med. *183*, 1797–1806.

Goodell, M.A., Rosenzweig, M., Kim, H., Marks, D.F., DeMaria, M., Paradis, G., Grupp, S.A., Sieff, C.A., Mulligan, R.C., and Johnson, R.P. (1997). Dye efflux studies suggest that hematopoietic stem cells expressing low or undetectable levels of CD34 antigen exist in multiple species. Nat. Med. *3*, 1337–1345.

Hendrikx, P.J., Martens, C.M., Hagenbeek, A., Keij, J.F., and Visser, J.W. (1996). Homing of fluorescently labeled murine hematopoietic stem cells. Exp. Hematol. *24*, 129–140.

Jones, R.J., Wagner, J.E., Celano, P., Zicha, M.S., and Sharkis, S.J. (1990). Separation of pluripotent haematopoietic stem cells from spleen colony-forming cells. Nature *347*, 188–189.

Kawamoto, S., Niwa, H., Tashiro, F., Sano, S., Kondoh, G., Takeda, J., Tabayashi, K., and Miyazaki, J. (2000). A novel reporter mouse strain that expresses enhanced green fluorescent protein upon Cre-mediated recombination. FEBS Lett. *470*, 263–268.

Lanzkron, S.M., Collector, M.I., and Sharkis, S.J. (1999). Homing of long-term and short-term engrafting cells in vivo. Ann. N Y Acad. Sci. *872*, 48–54.

Metcalf, D. (1971). Haematopoietic Cells (Amsterdam: North-Holland).

Metcalf, D. (1999). Stem cells, pre-progenitor cells and lineage-committed cells: are our dogmas correct? Ann. N Y Acad. Sci. *872*, 289–303.

Oostendorp, R.A., Ghaffari, S., and Eaves, C.J. (2000). Kinetics of in vivo homing and recruitment into cycle of hematopoietic cells are organ-specific but CD44-independent. Bone Marrow Transplant. *26*, 559–566.

Osawa, M., Hanada, K., Hamada, H., and Nakauchi, H. (1996a). Long-term lymphohematopoietic reconstitution by a single CD34-low/negative hematopoietic stem cell. Science *273*, 242–245.

Osawa, M., Nakamura, K., Nishi, N., Takahasi, N., Tokuomoto, Y., Inoue, H., and Nakauchi, H. (1996b). In vivo self-renewal of c-Kit+ Sca-1+ Lin(low/−) hemopoietic stem cells. J. Immunol. *156*, 3207–3214.

Parmar, K., Sauk-Schubert, C., Burdick, D., Handley, M., and Mauch, P. (2003). Sca+CD34− murine side population cells are highly enriched for primitive stem cells. Exp. Hematol. *31*, 244–250.

Scharenberg, C.W., Harkey, M.A., and Torok-Storb, B. (2002). The ABCG2 transporter is an efficient Hoechst 33342 efflux pump and is preferentially expressed by immature human hematopoietic progenitors. Blood *99*, 507–512.

Smith, L.G., Weissman, I.L., and Heimfeld, S. (1991). Clonal analysis of hematopoietic stem-cell differentiation in vivo. Proc. Natl. Acad. Sci. USA *88*, 2788–2792.

Spangrude, G.J., Heimfeld, S., and Weissman, I.L. (1988). Purification and characterization of mouse hematopoietic stem cells. Science *241*, 58–62.

Spangrude, G.J., Brooks, D.M., and Tumas, D.B. (1995). Long-term repopulation of irradiated mice with limiting numbers of purified